A validated antibody toolbox for ALS research

Riham Ayoubi[1,2], Emma J. MacDougall[1,2], Ian McDowell[1,2], Michael S. Biddle[3], Bárbara T. Ferreira[3], CongYao Zha[1,2], Marie-France Dorion[4], Jay P. Ross[5], Sara González Bolívar[1,2], Vera Ruiz Moleón[1,2], Charles Alende[1,2], Vincent Francis[1,2], Maryam Fotouhi[1,2], Mathilde Chaineau[1,4], Carol X.-Q. Chen[1,4], Valerio E.C. Piscopo[1,4], Vincent Soubannier[1,4], Tracy Keates[6], Wen Hwa Lee[6], Brian D. Marsden[7], Leonidas Koukouflis[7], Edvard Wigren[8], Carolyn A. Marks[8], Luke M. Healy[9], Patrick A. Dion[2], Guy A. Rouleau[1,2], Edward A. Fon[1,2], Harvinder S. Virk[3], Susanne Gräslund[8], Opher Gileadi[6,8], Aled M. Edwards[1], Thomas M. Durcan[1,4], Peter S. McPherson[1,2], Carl Laflamme[1,2,*]

Author affiliations:

[1]Structural Genomics Consortium, Montreal Neurological Institute-Hospital (The Neuro), McGill University, Montreal, H3A 2B4, Canada.

[2]Neurodegenerative Diseases Research Group, Department of Neurology and Neurosurgery, Montreal Neurological Institute-Hospital (The Neuro), McGill University, Montreal, H3A 2B4, Canada.

[3]NIHR Respiratory Biomedical Research Centre, Department of Respiratory Sciences, University of Leicester, Leicester, LE3 9QP, UK.

[4]Early Drug Discovery Unit (EDDU), Department of Neurology and Neurosurgery, Montreal Neurological Institute-Hospital (The Neuro), McGill University, Montreal, H3A 2B4, Canada.

[5]Department of Genetics, Stanford University School of Medicine, Stanford, CA, 94305, USA

[6]Structural Genomics Consortium, Nuffield Department of Medicine, University of Oxford, Oxford, OX3 7FZ, UK

[7]Nuffield Department of Medicine, University of Oxford, Oxford, OX3 7FZ, UK.

[8]Structural Genomics Consortium, Department of Medicine, Karolinska Institute, Solna, 171 76, Sweden

[9]Neuroimmunology Unit, Department of Neurology and Neurosurgery, Montreal Neurological Institute-Hospital (The Neuro), McGill University, Montreal, H3A 2B4, Canada.

[*]Corresponding author

E-mail: carl.laflamme@mcgill.ca

Running title: Validated antibodies for ALS-related proteins

Keywords: amyotrophic lateral sclerosis, antibody validation, Only Good Antibodies (OGA), YCharOS

Abstract

Genetic studies have identified hundreds of risk genes for neurodegenerative diseases, yet translating these variants into disease mechanisms remains limited by incomplete knowledge of the protein products. Here, we present the ALS-Reproducible Antibody Platform (ALS-RAP), a systematic effort to characterize 303 antibodies targeting 33 amyotrophic lateral sclerosis (ALS) risk genes: ACSL5, ALS2, ANG, ANXA11, ATXN2, C9orf72, CAV1, CCNF, CHCHD10, CHMP2B, FIG4, FUS, HNRNPA1, HNRNPA2B1, KIF5A, LGALS1, MATR3, NEK1, OPTN, PFN1, SETX, SIGMAR1, SOD1, SPG11, SQSTM1, TAF15, TARDBP, TBK1, TIA1, TUBA4A, UBQLN2, VAPB, and VCP using knockout-based characterization to identify high-quality reagents in common applications. Using these antibodies, we profiled protein expression across human iPSC-derived and primary neurological cell types. Protein-level analyses revealed diverse cell type-specific expression patterns, with subsets of ALS-associated proteins enriched in glial or neuronal populations. This work provides a validated antibody toolbox and ALS protein resource for translating genetic risk into mechanistic insights.

Introduction

Large-scale genome-wide association (GWAS) and genome sequencing studies have identified numerous risk loci across multiple neurodegenerative diseases. Recent GWAS studies identified 134 and 75 risk loci for Parkinson's[1,2] and Alzheimer's disease[3,4], respectively. At least 33 genes have been linked to familial and sporadic forms of amyotrophic lateral sclerosis (ALS),[5,6] a rare but devastating motor neuron disorder with extremely poor prognosis. Yet functional follow-up remains scarce, in part, because most risk genes lack validated protein tools, hindering hypothesis generation, mechanistic validation, and translation of genetic discoveries into disease biology.

ALS illustrates this gap clearly. While four ALS-linked genes—*SOD1*, *C9orf72*, *FUS*, and *TARDBP*—have received the most intensive study and corresponding PubMed entries, the remaining 29 ALS-associated proteins remain relatively underexplored in the context of the disease. An exception is an RNA-binding protein module that includes TDP-43, FUS, Matrin-3, HNRNPA1, and HNRNPA2B1, whose members have been shown to interact in published studies and confirmed by an unbiased proximity mapping in HEK293 cells.[7-9] Multiple cellular pathways have been implicated in ALS pathogenesis, including RNA metabolism, autophagy, and lysosomal function, but the contributions of ALS-linked proteins to these processes remain poorly defined.

To address this gap, we established the ALS-Reproducible Antibody Platform (ALS-RAP): a comprehensive, openly accessible resource of genetically validated antibody reagents and matched knockout (KO) cell lines. This project builds on the Antibody Characterization through Open Science (YCharOS) initiative, which systematically evaluates commercial antibodies. In collaboration with leading antibody manufacturers and KO cell lines providers, the YCharOS ecosystem developed a standardized, consensus KO-based characterization workflow.[10,11] Using this approach, high-quality renewable antibodies (monoclonal and recombinant) were shown to exist for a substantial fraction of the proteome—including understudied proteins—and recombinant antibodies consistently match or outperform traditional polyclonal and hybridoma-derived monoclonal reagents.[12] When gaps were identified, the Structural Genomics Consortium (SGC), an international public–private partnership dedicated to advancing our understanding of the human proteome, employed animal-free phage-display technology to generate single-chain variable fragment (scFv) recombinant antibodies optimized for recognizing native proteins.[13]

In this study, we characterized 303 antibodies targeting 33 ALS-associated proteins, evaluating their performance in western blotting (WB), immunoprecipitation (IP), and immunofluorescence (IF). KO-based characterization data were compiled into target-specific antibody characterization reports and deposited on Zenodo (zenodo.org/communities/ycharos), an open-access repository hosted by CERN; a subset was subsequently published as peer-reviewed articles in the *F1000Research* YCharOS Gateway

(f1000research.com/gateways/ycharos), which includes a dedicated ALS section. These datasets were further curated by the Only Good Antibodies (OGA) initiative and integrated into their reagent analysis platform (https://onlygoodantibodies.co.uk).[14] Collectively, these datasets constitute ALS-RAP, which serves as a validated resource to accelerate reproducible ALS research. We then used high-performing antibodies to profile protein expression across human induced pluripotent stem cell (iPSC)-derived and primary neurological cells. This effort revealed diverse and often unexpected cell type–specific expression patterns, including glial enrichment for 8 ALS-associated proteins, providing a new framework for exploring the cellular mechanisms underlying ALS.

Results

Genetic prioritization and initial characterization of ALS-RAP targets

We prioritized 33 ALS-related genes supported by replicated genetic evidence: *ACSL5*, *ALS2*, *ANG*, *ANXA11*, *ATXN2*, *C9orf72*, *CAV1*, *CCNF*, *CHCHD10*, *CHMP2B*, *FIG4*, *FUS*, *HNRNPA1*, *HNRNPA2B1*, *KIF5A*, *LGALS1*, *MATR3*, *NEK1*, *OPTN*, *PFN1*, *SETX*, *SIGMAR1*, *SOD1*, *SPG11*, *SQSTM1*, *TAF15*, *TARDBP*, *TBK1*, *TIA1*, *TUBA4A*, *UBQLN2*, *VAPB*, *VCP*. Building on a previous classification framework,[6] these genes were categorized into six groups based on variant frequency and estimated pathogenic impact: (1) rare variants with high effect size, (2) rare variants with intermediate effect size, (3) rare variants with small effect size, (4) rare variants with unknown effect size, (5) common variants with unknown effect size, and (6) common variants with small effect size. Of these, 25 genes have also been curated by the Clinical Genome Resource (ClinGen) expert panel for ALS spectrum disorders and were classified as having limited, moderate, or definitive evidence of association, whereas genes classified by ClinGen as refuted or disputed were not included in this study (Table 1).[15]

To estimate how well ALS-associated proteins are represented in the existing literature, PubMed searches were performed for each gene using either the gene name alone or in combination with the term “ALS” (Table 1, ordered by number of PubMed entries). The results, visualized as a line-scan plot (Figure S1), revealed that *SOD1*, *TARDBP*, *C9orf72*, and *FUS* dominate the field, accounting for 10,809 of 13,173 total publications (>80%) in the context of ALS, with *FUS* contributing the fewest among these four (1,332). In contrast, the remaining 29 genes are far less studied in ALS and collectively define what we refer to as the dark ALS-ome, referring to ALS-associated proteins with minimal functional characterization. Of these 29, seven genes—*VCP*, *OPTN*, *SQSTM1*, *TBK1*, *ANG*, *TIA1*, and *CAV1*—have attracted substantial attention in other biological contexts.

Reagent evaluation and antibody development for ALS-RAP targets

According to the CiteAb reagent database (citeab.com), only three of the 33 ALS-RAP targets have a top-cited renewable antibody that has been genetically validated using knockdown or KO approaches, revealing a substantial gap in validated reagents. We therefore sought to establish renewable antibody coverage across the entire target set. Before initiating antibody benchmarking using YCharOS protocols, we assessed the availability of renewable antibodies for all ALS-RAP targets using CiteAb, as batch-to-batch variability of polyclonal antibodies limits reproducibility.[12,16]

Six proteins—ANXA11, OPTN, MATR3, PFN1, UBQLN2 and VCP—had limited commercially renewable antibodies. To address this gap, the SGC generated scFv recombinant antibodies optimized for recognition of native, folded proteins, making them particularly suitable for IP.[13] Recombinant antigens were used for initial screening, and antibody-antigen bindings in cell lysates were assessed by IP coupled by

mass spectrometry (IP-MS) following established protocols.[17] For each target, at least three scFv clones were screened by IP-MS and the top-performing clone—selected solely on the basis of IP-MS enrichment—was benchmarked against available commercial antibodies. Antibody-encoding plasmids were deposited at Addgene, allowing researchers to produce these reagents independently.

In parallel, we evaluated KO cell line coverage for the 33 ALS-RAP targets to support antibody characterization. Twenty-one commercial KO lines were available from YCharOS partners in commonly used culture cell lines. These were selected based on parental expression levels above 2.5 $\log_2$(TPM+1) in the DepMap database—an expression threshold suitable for antibody characterization studies.[11] To complete coverage, 12 additional custom KO lines were generated and are available upon request, while *VCP* was targeted with siRNA as it is an essential gene.

Antibody performance and coverage for ALS-RAP proteins

We systematically characterized antibody performance for ALS-RAP proteins across WB, IP, and IF following KO-based consensus, industry-endorsed protocols.[11] In total, 303 antibodies (297 commercial and 6 custom scFv antibodies) targeting 33 ALS-associated proteins were evaluated. All antibodies were tested in WB across all targets. For five proteins—ALS2, FIG4, NEK1, SIGMAR1, and SPG11—IF was performed; however, under the standardized YCharOS conditions, signal intensity was indistinguishable between WT and KO cells and, in the absence of a validated reference antibody, performance could not be confidently assessed. These IF data were therefore not included in the Zenodo report, although successful detection under alternative, target-specific conditions cannot be excluded. In addition, antibodies against ANG, CAV1, CCNF, KIF5A, and SETX were not assessed in IP and/or IF due to the recent introduction of renewable reagents (limiting testing to WB), requirements for specialized experimental conditions (e.g., CCNF and cell-cycle arrest), and the secreted nature of ANG, which precluded IF testing (Figure 1A).

Across all 33 targets, at least one renewable, KO-validated antibody was identified for 32 (97%), 23 (70%), and 20 (61%) proteins in WB, IP, and IF, respectively (Figure 1B). Overall, 243 of 303 antibodies (80%) detected their intended target in WB, 105 of 238 (44%) immunoprecipitated their target, and 107 of 231 (46%) demonstrated specific target staining in IF (Figure 1C). The newly developed scFv antibodies filled key gaps; for example, the scFv against PFN1 was the only antibody—among 16 tested—capable of immunoprecipitating the protein.[20] Collectively, these results demonstrate that renewable, KO-validated antibodies cover most ALS-associated proteins, enabling reproducible studies of ALS biology.

We compiled 33 comprehensive antibody characterization reports, one report per protein, which were reviewed in collaboration with YCharOS industry partners, and published on Zenodo (https://zenodo.org/communities/ycharos/); 15 were subsequently published as peer-reviewed articles in *F1000Research* (f1000research.com/gateways/ycharos). All 303 antibodies evaluated in this study are listed in Table S1 (Supplementary Information), together with direct links to their corresponding

characterization reports. To enhance reagent traceability and reuse, we obtained Research Resource Identifiers (RRIDs) for all antibodies tested and KO cell lines used from the Antibody Registry and Cellosaurus databases,[18,19] which are cited in the corresponding antibody characterization reports. Antibodies used for downstream analyses of protein expression across neurological cell types were selected based on these validation data, prioritizing renewable and highly selective reagents. Catalogue numbers for these antibodies are provided in the Key Resources Table.

Antibody characterization case study: Galectin-1

A core objective of the ALS-RAP project is to generate high-quality antibody characterization datasets through systematic side-by-side testing. As an illustrative example of the YCharOS workflow, we present the antibody characterization for the Galectin-1 protein, encoded by the *LGALS1* gene. Galectin-1 is a lectin implicated in immune and stress responses in the nervous system and has been reported in association with ALS in prior transcriptomic and functional studies.[21,22] Antibodies were not assigned scores, consistent with the YCharOS philosophy that end users should evaluate raw data to select fit-for-purpose reagents based on their specific experimental needs.

The first step in the YCharOS pipeline is the selection of a cell line expressing the target protein at detectable levels. Transcriptomic data from the DepMap database indicate that the HAP1 cell line expresses *LGALS1* at 7.9 $\log_2$(TPM+1), well above the minimum expression threshold of 2.5 $\log_2$(TPM+1). An *LGALS1* KO HAP1 cell line was received in kind from Revvity. Notably, analysis of HAP1 exon sequencing data from DepMap confirmed that the parental HAP1 line does not harbor *LGALS1* variants that could interfere with antibody binding. A total of 10 commercial antibodies—all renewable—were obtained from YCharOS partners, Abcam (ab108389, ab138513, ab192842), ABclonal (A21218), Aviva Systems Biology (ARP58491_P050), Bio-Techne (MAB1152), Cell Signaling Technology (12936), and Thermo Fisher Scientific (MA5-32779, MA5-35566, MA5-47904). Antibodies are listed in Table 2.

To evaluate antibody performance in WB, protein lysates from WT and *LGALS1* KO HAP1 cells were resolved by SDS-PAGE, transferred to nitrocellulose membranes, and probed with each antibody in parallel (Figure 2A). This analysis confirmed the absence of detectable residual or truncated Galectin-1 protein in the KO cell line, a phenomenon observed in approximately 15% of commercial KO lines.[12] In this context, high-quality antibodies are expected to detect a specific signal in WT lysates with complete signal loss in KO lysates. Galectin-1 was detected in conditioned medium, and analysis of comparable amounts of protein from WT and KO lysates and media revealed similar intracellular and extracellular levels in HAP1 cells (Figure 2B).

Next, the ability of each antibody to capture Galectin-1 in IP was assessed, using 2 µg of each antibody, followed by WB analysis (Figure 2C). Equal amounts of starting material (SM), unbound fractions (UB), and IP eluates were resolved by SDS-PAGE. High-quality IP antibodies are expected to enrich Galectin-1 in the

IP fraction relative to the SM and to deplete the protein from the UB fraction, either partially or completely, depending on the incubation time of the lysate with the antibody and the target's abundance. Galectin-1 ranks among the top 5% most abundant proteins across many cell lines according to PaxDb (paxdb.org), and therefore partial depletion in the UB is expected.

Finally, antibody performance in IF was evaluated using a mosaic strategy. WT and *LGALS1* KO HAP1 cells were differentially labeled with fluorescent dyes, mixed, and imaged within the same field of view, thereby minimizing staining, imaging, and analysis bias. Quantitative analysis of fluorescence intensity was performed across hundreds of WT and KO cells for each antibody (not shown). Representative images are shown in Figure 2D and reflect the underlying quantitative measurements. All experimental data are compiled in a corresponding Zenodo report.

ALS-RAP antibody recommendations on the OGA website

In addition to primary data dissemination through YCharOS, each ALS-RAP antibody characterization study was independently evaluated by the OGA initiative, which did not participate in generating the ALS-RAP data. OGA integrates KO-based validation datasets generated by YCharOS into its publicly accessible antibody assessment platform (https://onlygoodantibodies.co.uk/), where reagents are curated, contextualized, and presented to support informed antibody selection by end users. The data is presented with easy access links to antibody purchasing pages from the manufacturer. A screenshot of the Galectin-1 dataset is shown as an illustrative example: schematic representations of high-quality antibodies are highlighted in the top row, while all tested antibodies are listed below in a randomized order, along with application-specific recommendations derived from OGA analysis of the YCharOS data (Figure 3).

OGA adds an interpretive layer to the YCharOS datasets by aggregating validation evidence across multiple applications and highlighting antibodies that demonstrate target specificity under defined experimental conditions. By cross-referencing ALS-RAP data within OGA, validated antibodies against ALS-associated proteins become more discoverable to non-specialist users, lowering barriers to reagent selection while preserving access to the underlying raw data. This complementary integration enhances the impact of ALS-RAP by pairing KO-based experimental validation with an accessible recommendation framework, thereby promoting reproducibility and responsible reagent use throughout the ALS research community.

Neurological expression scan of 30 ALS-RAP proteins

To provide contextual insight into the cellular distribution of ALS-associated genes, we examined cell type–specific RNA expression using the single-nuclei brain dataset from the Human Protein Atlas (HPA).[23] RNA enrichment was defined as a ≥1.5-fold increase relative to the average expression across all cell types in the dataset (motor neuron RNA data are not available in HPA), and genes were broadly categorized as neuron-enriched, glial-enriched (including astrocytes, oligodendrocytes and microglia), or broadly

expressed. A subset of genes showed preferential neuronal expression (ALS2, CCNF, KIF5A, and TUBA4A), whereas several others were enriched in glial populations (ACSL5, ANXA11, C9orf72, CAV1, CHMP2B, FIG4, FUS, HNRNPA1, LGALS1, SETX, SQSTM1, and TBK1). The remaining genes displayed broad expression, and four (ANG, MATR3, SIGMAR1, and TIA1) were weakly detected across neurological cell types. Overall, this RNA-based overview, together with a published single-cell RNA sequencing analysis of postmortem human brains,[24] highlights the heterogeneous and non-neuronal expression of ALS-associated genes and provides context for subsequent protein-level analyses (Figure S2).

Because RNA abundance does not necessarily predict protein levels,[25,26] we next examined ALS-RAP protein expression across neurological cell types using WB. We prioritized human iPSC-derived cells, as they provide experimentally tractable, reproducible, and relatively homogeneous populations for comparative analysis. Lysates were generated from iPSC-derived motor neurons, dopaminergic neurons, oligodendrocytes, astrocytes, and microglia using established differentiation protocols, as described in detail in the Methods section, with most cell types derived from the same healthy control iPSC line. Because differentiation protocols and donor genetic background can influence expression profiles, we complemented iPSC-derived cultures with primary human cells, including fetal astrocytes, fetal microglia, and monocyte-derived macrophages (MDMs).

The identity of each iPSC-derived cell population was assessed by gene expression analysis (not shown) and by WB for established lineage-specific marker proteins to evaluate culture purity. Motor neuron cultures selectively expressed the motor neuron marker ISL1 and the synaptic vesicle protein synaptotagmin-1 (SYT1), with no detectable signal for the pan-glial marker CD44. Dopaminergic neuron cultures expressed tyrosine hydroxylase (TH) together with SYT1. Oligodendrocyte cultures expressed myelin basic protein (MBP) and CD44, consistent with a glial lineage identity. Astrocyte and microglia cultures expressed their expected lineage markers (GFAP and CD44 for astrocytes; CD11b and Iba1 for microglia) (Figure S3). With cell identity and culture composition established, we next systematically examined ALS-RAP protein expression across these neurological cell types.

We profiled 30 ALS-RAP proteins by WB, with each target assessed using two independent preparations of the same cell types, one analyzed by chemiluminescence-based detection and the other by fluorescence-based WB. Three targets were excluded: CCNF, which requires cell-cycle arrest for reliable detection; ANG, which is secreted and therefore not readily detectable in cell lysates; and SETX, whose signal-to-noise ratio was insufficient for confident interpretation. Based on relative WB signal intensities across cell lineages and predefined enrichment thresholds, proteins were classified into three expression categories: 1) broadly expressed, 2) glial-enriched, or 3) neuron-enriched. Enrichment was defined as a ≥2.0-fold difference in fluorescence-based WB and a ≥2.5-fold difference in chemiluminescence-based WB between neuronal and glial groups (Table S2). Sixteen ALS-RAP proteins were detectably expressed across both neuronal and glial cell types and did not meet enrichment criteria in either group. This broadly

expressed group included CHMP2B, FIG4, FUS, HNRNPA1, MATR3, NEK1, OPTN, SIGMAR1, SOD1, SQSTM1, TAF15, TARDBP, TBK1, TIA1, UBQLN2, and VCP (Figure 4).

In contrast, eight ALS-RAP proteins exhibited preferential enrichment in glial cells, meeting enrichment thresholds in both detection modalities. These included ACSL5, ANXA11, C9orf72, CAV1, CHCHD10, LGALS1, PFN1 and SPG11. Aside from CAV1, these proteins showed the highest levels in iPSC-derived microglia, fetal microglia, and/or MDMs (Figure 5A). The neuron-enriched category comprised three proteins, ATXN2, TUBA4A, and VAPB, which displayed enrichment meeting threshold criteria relative to glial cells (Figure 5B). In addition, three ALS-RAP proteins, ALS2, HNRNPA2B1, and KIF5A, showed discordant enrichment patterns between the two independent experiments and were therefore classified as inconclusive (Figure 5C).

Overall, 13 of the 24 ALS-RAP targets that could be assessed at both the RNA and protein levels showed concordant cell type categorization between HPA RNA data and protein-level WB (Figure 5D). These protein-level analyses reveal substantial diversity in the cellular distribution of ALS-RAP proteins, and the enrichment of multiple ALS-associated proteins in myeloid and other glial populations underscores the potential contribution of non-neuronal cell types to ALS pathogenesis. Consistent with the limited availability of cell type–resolved protein data, STRING analysis of the 33 ALS-related proteins revealed sparse evidence of direct protein–protein interactions, with notable clusters among autophagy regulators (TBK1, OPTN, SQSTM1) and RNA-binding proteins (FUS, TARDBP, MATR3, HNRNPA1, and HNRNPA2B1) (Figure S4). Notably, these clusters comprise mostly broadly expressed proteins, increasing the likelihood that their interactions have been detected across multiple cellular contexts, whereas interactions involving more restricted ALS-RAP proteins may remain underexplored.

Discussion

Large-scale genetic studies have identified numerous risk genes across neurodegenerative diseases, including more than 30 genes linked to familial and sporadic ALS. However, for most of these genes, functional follow-up has lagged behind genetic discovery, largely due to the lack of validated protein reagents and systematic protein-level analyses. As a result, mechanistic insight has remained concentrated on a small subset of ALS genes, while the majority of ALS-associated proteins remain poorly characterized.

Here, we address this gap by leveraging the ALS-RAP, a comprehensive resource of KO-validated, renewable antibodies, to profile ALS-associated proteins across human neuronal and glial cell types. This work provides a protein-centric framework for interpreting ALS genetics and reveals widespread, and often unexpected, enrichment of ALS-associated proteins in glial and myeloid populations.

Although glial and immune mechanisms are increasingly implicated in ALS, most mechanistic studies have remained neuron-centric. While RNA sequencing has greatly advanced inference of cell type–specific expression, RNA abundance does not consistently predict protein levels, underscoring the need for direct proteomic validation. Using KO-validated renewable antibodies, we systematically profiled 30 ALS-associated proteins across iPSC-derived and primary neurological cell types and compared protein expression with RNA datasets. These analyses revealed that many ALS-associated proteins are enriched in glial populations, consistent with emerging evidence for non-neuronal contributions to ALS pathology, while also uncovering substantial RNA–protein discordance. Together, these findings highlight the importance of protein-level validation to refine transcriptomic predictions and improve the biological relevance of ALS disease models.

Despite strong genetic evidence implicating many ALS-associated genes, the majority of ALS-linked proteins remain part of the dark ALS-ome, with limited protein-level characterization across relevant cell types. Consistent with this gap, STRING network analysis revealed sparse connectivity among ALS-associated proteins, highlighting the need for orthogonal data to inform functional relationships. Here, our protein-level expression analysis identifies cell type–specific co-expression patterns that may help contextualize potential biological interactions. Notably, ANXA11, which encodes Annexin A11 and is classified as a definitive ALS gene by ClinGen, was predominantly expressed in microglial populations. Annexins are calcium- and phospholipid-binding proteins that regulate membrane curvature and participate in membrane trafficking and repair. However, despite emerging links between ANXA11 and autophagy or lysosomal homeostasis, its role in microglia or macrophages has not been systematically investigated. The microglial enrichment of ANXA11 observed here places it in the same cellular context as several ALS-associated proteins involved in autophagy and vesicular pathways, including C9orf72, TBK1, UBQLN2, SQSTM1, and OPTN, suggesting potential convergence on shared pathways in myeloid cells. Similarly, CHCHD10, classified as a moderate-confidence ALS gene by ClinGen, showed pronounced enrichment in

myeloid populations, despite the absence of studies examining its function in microglia or macrophages. In contrast, VAPB, a definitive ALS gene, displayed neuron-enriched expression, reinforcing its established association with neuronal biology and guiding mechanistic investigation toward neuron-intrinsic processes. Consistent with prior reports, C9orf72 was predominantly expressed in microglial populations. This observation aligns with recent studies implicating C9orf72 in microglial functions such as phagocytosis and immune regulation, and with emerging evidence suggesting that microglia may act as antigen-presenting cells in the central nervous system capable of activating $CD4^+$ T cells that recognize C9orf72-derived peptides.[27] Together, these findings support a model in which distinct subsets of ALS-associated proteins converge on cell type–specific pathways, underscoring the importance of protein-level, lineage-resolved analyses for elucidating ALS mechanisms.

Limitations of the study

This study focused on antibody reagents available within the YCharOS framework and did not systematically assess antibodies developed outside this ecosystem; consequently, additional high-quality renewable antibodies may exist that were not captured here. Protein expression profiling relied primarily on iPSC-derived neuronal and glial cell types, which offer experimentally tractable and relatively homogeneous populations but represent restricted developmental states and limited genetic diversity. Accordingly, the absence or low abundance of a given protein in these models should be interpreted with caution, as expression levels may differ in fully mature or regionally specialized cells *in vivo*. Differentiation efficiency and lineage purity can also vary across protocols and laboratories, potentially influencing relative expression patterns. Comparisons between iPSC-derived and primary cells likewise warrant careful interpretation; for example, ACSL5 was robustly expressed in fetal microglia but weaker in iPSC-derived microglia, whereas TARDBP showed the opposite pattern. Such differences likely reflect variation in developmental stage, culture conditions, and reprogramming-associated effects rather than true biological discrepancies. Finally, RNA-based analyses using the HPA dataset relied on predefined thresholds to infer cell type enrichment and were derived from independent samples rather than matched biological material, limiting direct quantitative comparison with protein-level data.

Resource availability

- All 33 ALS-RAP antibody characterization reports are publicly available on Zenodo, together with the complete raw characterization datasets (WB, IP, and IF, including Galectin-1): https://zenodo.org/communities/ycharos/
- A subset of 15 ALS-RAP targets has also been published in the *F1000Research* YCharOS Gateway and compiled within the dedicated ALS area: https://f1000research.com/gateways/ycharos/als
- Raw WB data supporting ALS-RAP protein expression profiling across neurological cell types are available on Zenodo.
    - The chemiluminescent-based experiment: https://doi.org/10.5281/zenodo.18484385
    - The fluorescent-based experiment: https://doi.org/10.5281/zenodo.18484483
- Curated YCharOS datasets, together with application-specific antibody recommendations, are accessible through the Only Good Antibodies (OGA) website: https://onlygoodantibodies.co.uk/

Acknowledgements

We would like to thank Kathleen Southern for the coordination of information exchange between laboratories involved in the ALS-RAP project. We would like to thank Abcam, ABCD Antibodies, ABclonal, Aviva System Biology, Cell Signaling Technology, Developmental Studies Hybridoma Bank, GeneTex, Revvity, Institute for Protein Innovation, MilliporeSigma, Novus Biologicals, Proteintech, R&D Systems, Thermo Fisher Scientific for providing antibodies and/or KO cell lines, free of charge, for ALS-RAP related targets. We would like to acknowledge the Birth Defects Research Laboratory, University of Washington, Seattle, USA for providing fetal tissues.

This work was supported by a grant from the Motor Neurone Disease Association, the ALS Association and ALS Canada to develop the ALS-Reproducibility Antibody Platform. This work was also supported by the Government of Canada through Genome Canada, Genome Quebec and Ontario Genomics (OGI-210) and by grant from the Quebec Consortium for Drug Discovery (CQDM), a grant from the Ministère de l'Économie, de l'Innovation et de l'Énergie du Québec. This work was supported by a grant from the National Centre for the Replacement, Refinement and Reduction of Animals in Research (NC3Rs) and MRC (NC3Rs Ref: NC/NAM0019/1, MRC UKRI076) alongside support from the Leicester Institute for Precision Health. The Structural Genomics Consortium is a registered charity (no. 1097737) that receives funds from Bayer, Boehringer Ingelheim, Bristol Myers Squibb, Genentech, Genome Canada through Ontario Genomics Institute (grant no. OGI-196), the European Union (EU) and European Federation of Pharmaceutical Industries and Associations through the Innovative Medicines Initiative 2 Joint Undertaking (EUbOPEN grant no. 875510), Janssen, Merck (also known as EMD in Canada and the USA), Pfizer and Takeda. R.A. is supported by a Mitacs postdoctoral fellowship. This work was supported by a CIHR project grant (PJT-195804). E.A.F. is supported by a Canada Research Chair (Tier 1) in Parkinson's disease. J.P.R. is supported by an ALS Scholars in Therapeutics postdoctoral fellowship from the Sean M. Healey & AMG Center for ALS at Massachusetts General Hospital (MGH), ALS FindingACure, and FightMND.

Author contribution

R.A., O.G., A.M.E., T.M.D., P.S.M., and C.L. conceived the study. I.M. analyzed ALS-RAP RNA sequencing data from the Human Protein Atlas. R.A., C.Z., S.G.B., V.R.M., C.A., and M.F. performed experiments and generated data. E.J.M., M.C., C.X.-Q.C., V.E.C.P., and V.S. generated iPSC-derived neurological cell types. M.S.G, B.T.F. and H.S.V established the Only Good Antibodies (OGA) website. T.K., W.H.L., E.W., and C.A.M. generated and characterized scFv antibodies. B.D.M. and L.K. established curated the ALS-RAP target list. M.-F.D. and L.M.H. isolated fetal astrocytes and fetal microglia and generated monocyte-derived macrophages. V.F., R.A., S.G.B and C.L. participated in data dissemination. P.A.D., J.P.R. and G.A.R. contributed to defining the initial ALS-RAP target list. R.A., I.M., and C.L. analyzed and interpreted the data. C.L., O.G., S.G., A.M.E., T.M.D., E.A.F. and P.S.M. provided resources and supervision. C.L. wrote the original draft of the manuscript with input from R.A., A.M.E. and P.S.M. All authors reviewed and approved the final manuscript.

Declaration of interests

The authors report no competing interests.

Supplemental information

Figures S1-S4

Table S1. List of 303 antibodies targeting ALS-RAP proteins evaluated in this study

Table S2. Quantification of chemiluminescence- and fluorescence-based WB

Figure legends

Figure 1: Summary of antibody performance for ALS-RAP proteins. (A) Overview of the identification of high-quality antibodies targeting ALS-RAP proteins. **(B)** Percentage of ALS-RAP targets covered by at least one specific renewable (monoclonal or recombinant) antibody for the indicated application. **(C)** Percentage of tested antibodies that met specificity criteria in each indicated application.

Figure 2: YCharOS antibody characterization workflow for Galectin-1 (*LGALS1*). Ten Galectin-1 antibodies were evaluated side-by-side across three applications using HAP1 WT and *LGALS1* KO cells. **(A)** Whole-cell protein lysates from HAP1 WT and *LGALS1* KO cells (20 µg per lane) were analyzed in WB using the indicated Galectin-1 antibodies. Ponceau-stained membranes are shown to assess protein loading and transfer efficiency. **(B)** Whole-cell protein lysates (10 µg) and conditioned media (10 µg) from HAP1 WT and *LGALS1* KO cells were analyzed in WB using antibody 12936, as in (A), to detect intracellular and secreted Galectin-1. **(C)** Immunoprecipitation was performed from HAP1 WT cell lysates using the indicated Galectin-1 antibodies. Starting material (SM), unbound fractions (UB), and whole immunoprecipitates (IP) were analyzed by WB. Anti-Galectin-1 antibody A21218 was used as a primary antibody. **(D)** HAP1 WT and *LGALS1* KO cells were differentially labeled with green and far-red fluorescent dyes, respectively, mixed at a 1:1 ratio, and plated in optically clear 96-well plates. Cells were stained with the indicated Galectin-1 antibodies, followed by Coralite 555–conjugated secondary antibodies and DAPI. Images were acquired in the blue (DAPI), green (WT), red (antibody staining), and far-red (KO) channels. Representative grayscale images of the blue and red channels are shown; WT and KO cells are outlined with green and magenta dashed lines, respectively. Scale bar, 10 µm. Recombinant antibodies are denoted by double asterisks (**) and monoclonal antibodies by single asterisks (*) after the catalogue numbers; polyclonal antibodies are unmarked. Antibody screening was performed in two independent experiments; representative data from one experiment are shown.

Figure 3: Accessing curated antibody characterization data through the OGA website. YCharOS antibody characterization data for ALS-RAP proteins are accessible through the Only Good Antibodies (OGA) website (https://onlygoodantibodies.co.uk/). The OGA homepage provides a searchable interface for the 33 ALS-RAP proteins, together with 35 additional neurological disease–associated proteins evaluated by YCharOS, and includes links to key OGA publications, data interpretation guidelines, antibody characterization protocols, and a portal for nominating new targets. **(A)** Representative results page generated by searching *LGALS1*, showing filters for host species, clonality, recombinant format, and OGA-recommended applications; the western blot (WB) filter is applied. A schematic panel at the top illustrates ideal antibody performance across applications, while antibodies matching the selected filters are displayed in randomized order. **(B)** Number of antibodies returned following application of the selected filters.

Figure 4: WB analysis of broadly expressed ALS-RAP proteins. WB showing 16 ALS-RAP proteins with broad cellular distribution across human-derived cell types. For each protein, two independent experiments are shown, with chemiluminescence-based WB (top) performed using a single shared lysate batch across all proteins and fluorescence-based WB (bottom) performed using a second, independent lysate batch shared across all corresponding WB. Broad expression was defined by the absence of consistent protein enrichment across both detection modalities relative to other cell types. Lysates were prepared from the indicated human iPSC-derived cell types, and proteins are listed in alphabetical order. A representative Ponceau-stained membrane is shown to assess protein loading and transfer efficiency. Vertical lines between the motor neuron and DA neuron lanes indicate that WB were spliced to remove additional conditions not relevant to this study. DA, dopaminergic. 1, motor neurons; 2, DA neurons; 3, oligodendrocytes; 4, astrocytes; 5, microglia.

Figure 5: Identification of glial- and neuronal-enriched ALS-RAP proteins by WB. WB analysis of ALS-RAP proteins exhibiting cell type–enriched expression patterns. **(A)** Eight glial-enriched ALS-RAP proteins and **(B)** Three neuronal-enriched ALS-RAP proteins analyzed across iPSC-derived cell types and primary cells. WB were generated using the same independent lysate batches, detection modalities, and visual presentation as in Figure 4. iPSC-derived neurological cell types were grouped into neuronal or glial categories. Enrichment was defined by reproducible, category-specific WB signals across independent experiments (see Methods). **(C)** WB analysis of three ALS-RAP proteins showing discordant cell type expression between the two independent experiments. Vertical lines between the motor neuron and DA neuron lanes indicate that WB were spliced to remove additional conditions not relevant to this study. In panel (A), fetal astrocyte lysates are absent for the CHCHD10 and SPG11 WB in the chemiluminescence-based experiment, as indicated by white boxes, and for LGALS1, PFN1, and SPG11 in the fluorescence-based experiment due to limited sample availability. **(D)** Summary of 13 targets for which WB data and Human Protein Atlas RNA expression profiles are concordant, grouped by expression category. DA, dopaminergic; MDM, monocyte-derived macrophages. *, band non-specific to C9orf72. 1, motor neurons; 2, DA neurons; 3, oligodendrocytes; 4, astrocytes; 5, microglia; 6, fetal astrocytes; 7, fetal microglia ; 8, MDMs.

Figure S1: Characterization of ALS-RAP targets. Number of PubMed entries related to ALS-RAP genes. Black points represent the number of entries retrieved using the search term “gene name + ALS,” while gray points represent entries retrieved using the gene name alone. The x-axis indicates the number of PubMed entries, and the y-axis lists the gene names.

Figure S2: ALS-RAP RNA expression across brain cell types. Heatmap showing normalized RNA expression values from the Human Protein Atlas (HPA) single nuclei brain dataset. Expression is given as nTPM values on a scale from 0-500. Genes denoted with an asterisk (*) are classified as “barely detectable” but show substantial expression in a single cell type.

Figure S3: Protein-level characterization of iPSC-derived neurological cells. (A) Table listing cell type–specific marker proteins. **(B)** WB analysis of marker proteins using antibodies against the indicated proteins. A Ponceau-stained membrane is shown to assess protein loading and transfer efficiency. Lysates were prepared from the indicated human iPSC-derived cell types or fetal astrocyte culture. Vertical lines between the motor neuron and DA neuron lanes and between the DA neuron and microglia lanes indicate that WB were spliced to remove additional conditions not relevant to this study. DA, dopaminergic; NPC, neuronal progenitor cells.

Figure S4: STRING analysis of known physical interactions between ALS-RAP proteins.

Table 1

Gene name	UniProt ID	Effect size (variants; effect size)	ClinGen curated description	PubMed entries (Gene name + ALS)	PubMed entries (Gene name)
SOD1	P00441	Rare; high	Definitive	4679	10855
TARDBP	Q13148	Rare; high	Definitive	2846	5061
C9orf72	Q96LT7	Rare; high	Definitive	1952	2757
FUS	P35637	Rare; high	Definitive	1332	5694
VCP	P55072	Rare; high	Definitive	267	2354
OPTN	Q96CV9	Rare; high	Definitive	206	1640
SQSTM1	Q13501	Rare; intermediate	Moderate	183	3848
TBK1	Q9UHD2	Rare; high	Definitive	178	2749
VAPB	O95292	Rare; intermediate	Definitive	169	417
ATXN2	Q99700	Rare; intermediate	Definitive	163	437
UBQLN2	Q9UHD9	Rare; high	Definitive	139	206
ALS2	Q96Q42	Rare; intermediate	Definitive	127	250
ANG	P03950	Rare; intermediate	Limited	99	1592
SETX	Q7Z333	Rare; intermediate	Not available	93	257
CHCHD10	Q8WYQ3	Rare; intermediate	Moderate	93	174
HNRNPA1	P09651	Rare; unknown	Not available	91	574
PFN1	P07737	Rare; intermediate	Definitive	79	356
TAF15	Q92804	Rare; intermediate	Limited	66	251
NEK1	Q96PY6	Rare; high	Definitive	64	192
MATR3	P43243	Rare; unknown	Definitive	61	162
KIF5A	Q12840	Rare; intermediate	Definitive	61	259
CHMP2B	Q9UQN3	Rare; intermediate	Definitive	48	225
TIA1	P31483	Rare; intermediate	Limited	47	1146
ANXA11	P50995	Rare; intermediate	Definitive	47	124
CCNF	P41002	Rare; small	Limited	41	184
FIG4	Q92562	Rare; intermediate	Limited	40	170
HNRNPA2B1	P22626	Rare; unknown	Moderate	38	535
SPG11	Q96JI7	Rare; intermediate	Definitive	34	283
TUBA4A	P68366	Rare; high	Moderate	32	95
SIGMAR1	Q99720	Rare; unknown	Not available	27	202
CAV1	Q03135	Rare; small	Limited	14	6065
ACSL5	Q9ULC5	Common; small	Not available	4	192
LGALS1	P09382	Rare; high	Not available	3	308

Table 2

Company	Catalog number	Lot number	RRID (Antibody Registry)	Clonality	Clone ID	Host	Concentration (µg/µL)	Vendors recommended applications
Abbexa	abx349932**	A2510972L	NA	recombinant mono	F704	mouse	0.86	Other
Abcam	ab108389**	1018000-29	AB_10863417	recombinant mono	EPR3205	rabbit	1.35	Wb, IF
Abcam	ab138513*	1086382-8	AB_2894851	monoclonal	EPR3206(2)	rabbit	0.26	Wb, IF
Abcam	ab192842**	1011456-2	NA	recombinant mono	SP247	rabbit	0.04	Wb
ABclonal	A21218**	3522042922	NA	recombinant mono	ARC53156	rabbit	1.20	Wb
Aviva Systems Biology	ARP58491_P050	QC25810-42978	AB_2046045	polyclonal	-	rabbit	0.50	Wb
Bio-Techne (R&D Systems)	MAB1152*	CJKC0325011	AB_3657585	monoclonal	933133	mouse	0.50	Wb
Cell Signaling Technology	12936**	3	AB_2798065	recombinant mono	D608T	rabbit	0.10	Wb, IF
Thermo Fisher Scientific	MA5-32779**	79527780	AB_2810056	recombinant mono	JM13-37	rabbit	1.00	Wb, IP, IF
Thermo Fisher Scientific	MA5-35566**	79531623	AB_2849466	recombinant mono	7W5Q6	rabbit	2.00	Wb, IF
Thermo Fisher Scientific	MA5-47904**	79531680	AB_3074348	recombinant mono	SAIC-25B-112	rabbit	1.00	Wb

Methods

Analysis of PubMed entries for each ALS-associated gene

Throughout the manuscript, we reference ALS-RAP targets using their official gene names as listed in UniProt, written in italics (e.g., *SOD1*). To refer to the corresponding proteins, we use the same gene names in regular font, as the official protein names are often too long or ambiguous for practical use.

Each target gene was queried in PubMed using two search strategies: (1) GENE_NAME[Title/Abstract] to retrieve the total number of publications associated with the gene, and (2) (GENE_NAME[Title/Abstract]) AND ("amyotrophic lateral sclerosis" [Title/Abstract]) to identify publications specifically linking the gene to ALS. Searches were performed on August 27, 2025.

Evaluation of significance of ALS-associated genes

Each candidate gene was assessed for its potential association with ALS using the evidence published at the time of this manuscript. Using the recent review of Nijs & van Damme as a model,[6] we used currently available evidence to prioritize genes for potential association with ALS in a similar manner. First, genes were qualitatively assessed for rarity of genetic variants in the general population and among individuals with ALS. Next, any reported odds ratios (OR) for risk of ALS in variant carriers were used to approximate whether genes could be considered as having "small" (OR < 1.2), "intermediate" (1.2 < OR < 10), or "high" (OR > 10) effect sizes. Genes were assigned an "uncertain" OR estimate if no OR had been published at the time of analysis. Variant frequency was assessed considering the type(s) of inheritance previously described; variants reported through GWAS or genotyping studies were designated as "common" whereas variants reported in autosomal family/pedigree-based studies were designated as "rare". If the method of discovery was poorly described or through non-genetic analyses (e.g. transcriptomic or proteomic), genes were described as having "uncertain" frequency.

RNA expression analysis

We accessed the single-cell transcriptomics resource of the Human Protein Atlas (HPA), specifically the single-nuclei brain dataset which includes single-cell RNA sequencing data generated from 2.5 million cells and mapped to 34 supercluster cell types. Data were generated from post-mortem human brain samples digested to a single cell suspension, and cell types were clustered into transcriptomic cell types.[28] Raw sequencing data was normalized using Trimmed mean of M values and expression values were presented as normalized transcripts per million (nTPM). RNA expression data for all 33 ALS genes were downloaded online from the HPA. Data were grouped together based on overall cell type (neuron, oligodendrocyte, astrocyte, microglia, etc.) and the average expression in each cell type was determined for each gene. The average neuron, oligodendrocyte, astrocyte, and microglia expression data were extracted from the overall dataset and used in downstream analyses.

In our analyses, genes were considered “expressed” if their expression values in at least three cell types were greater than the median expression value of the entire HPA dataset (9.2 nTPM). Genes were considered “barely detectable” if expression was less than the median value in at least two cell types. For a small subset of “barely detectable” genes, expression in one cell type was greater than the median value and substantially “enriched” in that cell type. We included these in the category of “expressed” genes despite the low expression in most cell types.

To describe the cell type expression patterns for each gene, we established criteria determining if mRNA expression levels for a gene is “enriched” or not in a given cell type. Cell types in which mRNA expression for a gene is “enriched” were defined as when the ratio of the expression value in that cell type to the average expression value across all cell types was greater than or equal to 1.5*. Each gene was categorized based on the “enriched” cell types. If either more than one cell type was “enriched” or no cell types were, the gene was categorized as having “low cell-type specificity”.

$$*\frac{Expression\ value\ in\ given\ cell\ type}{Average\ across\ all\ cell\ types} \geq 1.5$$

String analysis

STRING analysis was performed by entering the UniProt IDs of the 33 ALS-RAP proteins into the “multiple proteins” search at string-db.org. The analysis was restricted to the “physical subnetwork”, with the meaning of network edges set at “confidence”, and the minimum required interaction score set to “highest confidence”.

Western blot (WB)

Primary cells, iPSC-derived cultures and cultured cells were collected in RIPA buffer (25mM Tris-HCl pH 7.6, 150mM NaCl, 1 % NP-40, 1% sodium deoxycholate, 0.1% SDS) supplemented with protease inhibitors. Lysates were sonicated briefly for 5-10 secs depending on the volume. Following 30 min on ice, lysates were spun at ~110,000 x *g* for 15 min at 4°C and equal protein aliquots of the supernatants were analyzed by SDS-PAGE and WB.

Chemiluminescent WB

WB were performed with precast 10% Bis-Tris polyacrylamide gels (MOPS or MES buffer) and nitrocellulose membranes. Total proteins were visualized with a Ponceau staining. Blots were blocked with 5% milk in TBS with 0.1% Tween 20 (TBST). Antibodies were also diluted in 5% milk in TBST and incubated O/N at 4°C. Membranes were washed three washes in TBST the next day. The peroxidase conjugated anti rabbit and anti-mouse secondary antibodies (Thermo Fisher Scientific) were diluted in 5% milk in TBST at 0.5 and 1 µg/mL, respectively. Secondaries were incubated with the membranes for 1 hr at room temperature followed by three washes. Membranes were incubated with ECL for 1 min prior to detection with the iBright CL1500 Imaging System (Thermo Fisher Scientific).

Fluorescent WB

WB were performed with large 5–16% gradient Tris-based polyacrylamide gels (Tris-Glycine/SDS Buffer) and nitrocellulose membranes. Total proteins were visualized with the REVERT total protein stain (LI-COR Biosciences). Blots were blocked with 5% milk in TBST, and antibodies were diluted in the same buffer and incubated O/N at 4°C followed by three washes. The secondary antibodies (Odyssey IRDye 800CW or IRDye 680RD) were diluted in 5% milk in TBST to a final concentration of 0.05 µg/mL for anti-rabbit and 0.1 µg/mL for anti-mouse. Secondaries were incubated with the membranes for 1 hr at room temperature followed by three washes while covered from the light. Immuno-reactive bands were detected using the LI-COR Odyssey Imaging System (LI-COR Biosciences), and data analysis was done using LI-COR Image Studio Lite Version 6.10.2.

Galectin-1 antibody screening in WB

For cell lysis, HAP1 WT and *LGALS1* KO cells were collected in RIPA buffer and processed as described above.

To collect the conditioned medium, HAP1 WT and *LGALS1* KO cells were washed 3x with PBS 1x and starved for ~36 hrs in Iscove's Modified Dulbecco's Medium (IMDM) supplemented with 1% Pen/Strep and 1% L-Glutamine. Culture media were collected and centrifuged for 10 min at 500 x *g* to eliminate cells and larger contaminants, then for 10 min at 4,500 x *g* to eliminate smaller contaminants. Culture media were then concentrated by centrifuging at 4,000 x *g* for 30 min using the Amicon Ultra-15 Centrifugal Filter Units with a membrane NMWL of 10kDa. Culture media were finally supplemented with 1x protease inhibitor cocktail mix.

10% Bis-Tris gels with MES buffer were used for SDS-PAGE and western blot was performed using the primary antibodies (Table 2) at the following dilutions: ab108389 at 1/100, ab138513 atv1/10 000, ab192842 at 1/100, A21218 at 1/11 000, ARP58491 at 1/100, MAB1152 at 1/250, 12936 at 1/1000, MA5-32779 at 1/2000, MA5-35566 at 1/200, MA5-47904 at 1/1000. Anti-rabbit and anti-mouse antibodies (Proteintech) were used at a final concentration of 0.05 µg/ml and 0.5 µg/ml, respectively.

Galectin-1 antibody screening in immunoprecipitation (IP)

Antibody-bead conjugates were prepared by adding 2 µg to 500 µl of Pierce IP Lysis Buffer from Thermo Fisher Scientific in a microcentrifuge tube, together with 30 µl of Dynabeads protein A- (for rabbit antibodies). Tubes were rocked for 1 h at 4°C followed by two washes to remove unbound antibodies. HAP1 WT were collected in Pierce IP buffer (25 mM Tris-HCl pH 7.4, 150 mM NaCl, 1 mM EDTA, 1% NP-40 and 5% glycerol) supplemented with protease inhibitor. Lysates were rocked 30 min at 4°C and spun at 110,000 x *g* for 15 min at 4°C. 0.2 ml aliquots at 1 mg/ml of lysate were incubated with each antibody-bead conjugate for 2 h at 4°C. To run 4% SM alongside each IP on the gel (8 µl per SM), a master mix of lysate

was kept aside on ice for subsequent SM sample preparation. The UBs were collected separately and prepared for gel loading similar to the rest of the samples. Beads were washed three times with 1.0 ml of IP buffer and processed for SDS-PAGE on precast midi 10% Bis-Tris polyacrylamide gels. For WB, membranes were trimmed at 24 kDa and the lower part was incubated with the rabbit recombinant monoclonal anti-Galectin-1 antibody A21218 diluted at 1/3000 in 5% milk in TBST. HRP-conjugated anti-rabbit (Proteintech) diluted in 5% milk in TBST was used as a secondary antibody at 0.05 µg/ml.

Galectin-1 antibody screening in immunofluorescence (IF)

WT and *LGALS1* KO HAP1 cells were labelled with a green and a far-red fluorescence dye, respectively. WT and KO cells were plated 96-well plate with optically clear flat-bottom (Perkin Elmer) as a mosaic and incubated for 24 hrs in a cell culture incubator at 37ºC, 5% CO2. Cells were fixed in 4% paraformaldehyde (PFA) in phosphate buffered saline (PBS). Cells were permeabilized in PBS with 0.1% Triton X-100 for 10 min at room temperature and blocked with PBS with 5% BSA, 5% goat serum and 0.01% Triton X-100 for 30 min at room temperature. Cells were incubated with IF buffer (PBS, 5% BSA, 0.01% Triton X-100) containing the primary Galectin-1 antibodies overnight at 4°C. Cells were then washed 3 × 10 min with IF buffer and incubated with the corresponding CoraLite Plus 555 secondary antibody in IF buffer at a dilution of 0.5 µg/ml for 1 hr at room temperature. Cells were washed 3 × 10 min with 1x PBS. The nuclei were labelled with DAPI fluorescent stain at a concentration of 5 ng/ml in 1x PBS for 3 min then washed once with 1x PBS.

Images were acquired on an ImageXpress micro confocal high-content microscopy system (Molecular Devices). The objective used is a water Apo LambdaS LWD with magnification of 20x, NA 0.95 and scientific CMOS cameras, equipped with 395, 475, 555 and 635 nm solid state LED lights (lumencor Aura III light engine) and bandpass filters to excite DAPI, Cellmask Green, Coralite-555 and Cellmask Red, respectively. Images had pixel sizes of 0.68 x 0.68 microns, and a z-interval of 4 microns. For analysis and visualization, shading correction (shade only) was carried out for all images. Then, maximum intensity projections were generated using 3 z-slices. Segmentation was carried out separately on maximum intensity projections of Cellmask channels using CellPose 1.0, and masks were used to generate outlines and for intensity quantification.

iPSC differentiation protocols

Healthy control iPSCs from the AIW002-02 & QPN929 backgrounds (Early Drug Discovery Unit-EDDU, McGill University) were selected for differentiation into the indicated neurological cell types. In all cases, iPSCs were cultured in mTeSR1 for 5-7 days prior to differentiation. Two batches of neurological cells were generated from the AIW002-02 background using identical protocols, with the exception that the QPN929 iPSC line was used for microglia differentiation in batch used for chemiluminescent western blotting.

Motor neuron differentiation

Motor neurons were differentiated from iPSCs following a previously published protocol.[29,30] Basic neural medium (BNM, 1:1 mixture of DMEM/F12 and Neurobasal, 0.5X N2, 0.5X B27, 0.5X GlutaMAX, 1X antibiotic-antimycotic, and 100 μM ascorbic acid) serves as the base medium for all other formulations used in this protocol. iPSCs were seeded on matrigel coated flasks in neural induction medium (BNM supplemented with 2 μM SB431542, 2 μM DMH1, 3 μM CHIR99021) with a full media change performed every other day. After 6 days, cells were passaged in patterning medium (BNM supplemented with 1 μM CHIR99021, 2 μM SB431542, 2 μM DMH1, 0.1 μM retinoic acid (RA) and 0.5 μM purmorphamine (PMN)) onto poly-L-ornithine- and laminin-coated flasks and cultured for a further 6 days with a full media change performed every other day. Cells were then passaged onto poly-L-ornithine- and laminin-coated flasks in expansion medium (BNM supplemented with 3 μM CHIR99021, 2 μM SB431542, 2 μM DMH1, 0.1 μM RA and 0.5 μM PMN, and 0.5 mM valproic acid (VPA)), with a full media change performed every other day for 6 days to obtain motor neural progenitor cells (M-NPCs). M-NPCs were dissociated as single cells and seeded onto poly-L-ornithine- and laminin-coated plates in final differentiation medium (BNM supplemented with 0.5 μM RA, 0.1 μM PMN, 0.1 μM Compound E (CpdE), 10 ng/mL insulin-like growth factor-1 (IGF-1), brain-derived neurotrophic factor (BDNF), and ciliary neurotrophic factor (CNTF)), with a half media change once per week for final differentiation into motor neurons (MNs). MNs were considered mature and collected for WB after four weeks of differentiation.

Dopaminergic neuron differentiation

Dopaminergic neurons were differentiated from iPSCs following a protocol of floor-plate induction with additional modifications.[31,32] Briefly, iPSCs were dissociated into single cells to form embryoid bodies (EBs). EBs were grown on low-attachment plates for one week in DMEM/F12 supplemented with 1X N2 and 1X B27, in the presence of 10 μM SB431542, 200 ng/mL Noggin, 200 ng/mL sonic hedgehog, 3 μM CHIR99021 and 100 ng/mL Fibroblast growth factor 8 (FGF8). On day 7, EBs were transferred, in the same media, to poly-L-ornithine- and laminin-coated plates. On day 14, rosettes were selected semi–manually and cultured as a monolayer in DMEM/F12 supplemented with 1X N2 and 1X B27 on poly-L-ornithine- and laminin-coated plates to generate dopaminergic neural progenitor cells (DA-NPCs). DA-NPCs were passaged at a ratio of 1:3 every 5-7 days. DA-NPCs were then cultured in neurobasal medium, supplemented with 1X N2 and 1X B27, in the presence of 1 μg/mL laminin, 500 μM dibutyryl-cAMP (db-cAMP), 20 ng/mL BDNF, 20 ng/mL glial-derived neurotrophic factor (GDNF), 200 μM ascorbic acid, 100 nM CpdE and 1 ng/mL transforming growth factor β3 (TGF-β3), with a half media change twice per week for final differentiation into dopaminergic neurons. Dopaminergic neurons were considered mature and collected for WB after four weeks of differentiation.

Oligodendrocyte differentiation

Oligodendrocytes were differentiated from iPSCs following a recently published protocol.[33] The base media for all other formulations in this protocol is as follows: DMEM/F12 with Glutamax supplemented with

1X N2, 1X B27, 1X NEAA, 55 mM b-mercaptoethanol, 25 mg/mL Insulin, and 2 mg/mL heparin. First, iPSCs were directed toward a neural progenitor fate in base media supplemented with 10 µM SB31542 and 2 µM DMH1, with daily media change over eight days. Followed by patterning with 100 nM RA and 1 µg/mL PMN in base media with daily media change, for four days. Cells were then transferred from monolayer to suspension culture in the same medium for an additional eight days to form neurospheres. Oligodendrocyte precursor cells (OPCs) were then generated and expanded in suspension using OPC media (base media supplemented with 10 ng/mL PDGF-AA, 10 ng/mL IGF-1, 10 ng/mL NT-3, 5 ng/mL HGF, 60 ng/mL 3, 3′, 5-Triiodo-L-thyronine (T3), 100 ng/mL biotin, and 1 µM db-cAMP) for 10 days. Following this, the cells were plated in OPC media onto poly-L-ornithine/laminin-coated vessels with half media changes performed every other day to support further differentiation toward the OPC lineage, which continues until day 75. At this stage, cells were detached and passaged using TrypLE™ Express Enzyme. In the final differentiation step, cells were exposed to ScienCell Astrocyte Medium supplemented with ScienCell Astrocyte Growth Supplements (AGS) for 10 days. AGS was then withdrawn, and final maturation completed by reintroducing IGF-1 and T3 at the previously described concentrations for a further 10 days, with half media changes performed every other day. At this point, oligodendrocytes were considered mature and collected for WB.

Astrocyte differentiation

Astrocytes were differentiated from iPSCs following a previously published protocol.[34] First, iPSCs were differentiated into neural progenitor cells following the steps described above for the generation of M-NPCs. M-NPCs were dissociated as single cells and plated at a low cell density (15,000 cells/cm^2) onto a matrigel coated vessel in M-NPC expansion media (as described above). The next day, medium was replaced with Astrocyte Differentiation Medium (ScienCell Astrocyte Medium containing AGS, 1% fetal bovine serum (FBS) (ScienCell Research Laboratories), 1% penicillin streptomycin (Wisent Bioproducts)). Cells were passaged in the same media at a ratio of 1:2 once per week and were maintained under these culture conditions for 30 days, with a half media change performed every 3-4 days. FBS was then withdrawn to promote astrocyte maturation. Cells were maintained for an additional four weeks with a half media change performed twice per week prior to astrocyte collection for WB.

Microglia differentiation

iPSC-derived microglia were differentiated following a published protocol.[35] Briefly, iPSCs were differentiated to hematopoietic precursor cells (iHPCs) using the STEMCELL Technologies STEMdiff™ Hematopoietic Kit. iHPCs were harvested on days 10 and 12 of iHPC differentiation and seeded on matrigel-coated 6-well plates in microglia differentiation media (MDM, DMEM/F12 HEPES no phenol red supplemented with 2X Insulin-transferrin-selenite, 2X B27, 0.5X N2, 1X Glutamax, 1X NEAA, 400 µM monothioglycerol, and 5 µg/mL insulin) + three cytokine cocktail (25 ng/mL M-CSF, 100 ng/mL IL-34, and 50 ng/mL TGF-β1) for further differentiation into microglia. Cells were supplemented with MDM + three cytokine cocktail every other day, with a full media change performed on day 12, for 24 days of iMG

differentiation. On day 25 a full media change to MDM + five cytokine cocktail (25 ng/mL M-CSF, 100 ng/mL IL-34, 50 ng/mL TGF-β1, 100 ng/mL CD200, and 100 ng/mL CX3CL1) was performed, followed by supplementation with MDM + five cytokine cocktail on day 27. Microglia were considered mature and utilized for downstream experiments after 28 days of microglial differentiation.

WB quantification

Chemiluminescence- and fluorescence-based WB were performed as independent experiments and analyzed separately. Band intensity quantification for iPSC-derived cell lines was performed using LI-COR Image Studio Lite software for all WB. Chemiluminescent images were converted to grayscale prior to quantification. For each lane, a rectangular region of interest was defined around the band(s) corresponding to the protein of interest, as identified by the loss of signal in KO-based validation within the YCharOS reports. Signal intensity was calculated by summing pixel intensities within each region and subtracting background signal, defined as the product of background intensity and region area.

The five iPSC-derived cell types were grouped into neuronal and glial categories. The neuronal group comprised motor neurons and dopaminergic neurons, whereas the glial group included oligodendrocytes, astrocytes, and microglia. For each protein, the highest quantified signal within one group was divided by the highest signal observed in the opposite group to calculate an enrichment ratio. For example, in fluorescence-based WB, ANXA11 showed a maximal signal of 16.1 in microglia and 4.1 in dopaminergic neurons, corresponding to a 3.9-fold enrichment in glial cells. Proteins with enrichment ratios ≥2.0 in fluorescence-based WB were classified as enriched in the corresponding cell group, whereas proteins with ratios below this threshold across all cell types were considered broadly expressed. For chemiluminescence-based WB, a higher enrichment threshold of 2.5 was applied. This difference reflects the linear signal detection of fluorescence-based WB compared with the logarithmic signal response of chemiluminescence resulting from horseradish peroxidase (HRP)-mediated enzymatic amplification.

Key resources table

REAGENT or RESOURCE	SOURCE	IDENTIFIER
Antibodies		
HRP-Goat polyclonal anti-Rabbit antibody Secondary Antibody (H+L)	Thermo Fisher Scientific	CAT# 65-6120; RRID: AB_2533967
HRP-Goat polyclonal anti-Mouse antibody Secondary Antibody (H+L)	Thermo Fisher Scientific	CAT#62-6520; RRID:AB_2533947
IRDye® 680CW Goat polyclonal anti-Rabbit Secondary Antibody (H+L)	LI-COR Biosciences	CAT#926-68071; RRID:NA
IRDye® 680CW Goat polyclonal anti-Mouse Secondary Antibody (H+L)	LI-COR Biosciences	CAT#926-68070; RRID:NA
IRDye® 800CW Goat polyclonal anti-Rabbit Secondary Antibody (H+L)	LI-COR Biosciences	CAT#926-32211; RRID:NA
IRDye® 800CW Goat polyclonal anti-Mouse Secondary Antibody (H+L)	LI-COR Biosciences	CAT#926-32210; RRID:NA
HRP-Goat multiclonal recombinant anti-Rabbit Secondary Antibody (H+L)	Proteintech	CAT#RGAR001; RRID:AB_3073505

HRP-Goat multiclonal recombinant anti-Mouse Secondary Antibody (H+L)	Proteintech	CAT#RGAM001; RRID: AB_3068333
CoraLite Plus 555-Goat multiclonal recombinant Anti-Rabbit Secondary Antibody (H+L)	Proteintech	CAT# RGAR003; RRID: AB_3073507
CoraLite Plus 555-Goat multiclonal recombinant Anti-Mouse Secondary Antibody (H+L)	Proteintech	CAT# RGAM003; RRID: AB_3068539
Rabbit recombinant monoclonal anti-CHMP2B (clone JE54-35)	Thermo Fisher Scientific	CAT#MA5-36184; RRID:AB_2890433
Rabbit recombinant monoclonal anti-FIG4 (clone N202/7R)	Addgene	CAT#192037; RRID:AB_2916241
Mouse monoclonal anti-FUS (clone CL0190)	Abcam	CAT#ab154141; RRID:AB_2885092
Mouse monoclonal anti-HNRNPA1 (Clone 4B10)	Bio-Techne (Novus Biologicals)	CAT#NB100-672; RRID:AB_524308
Rabbit recombinant monoclonal anti-MATR3 (clone EPR10634(B))	Abcam	CAT#ab151739; RRID:AB_2885091
Rabbit polyclonal anti-NEK1	GeneTex	CAT#GTX130828; RRID:AB_2886357
Mouse monoclonal anti-OPTN (clone 6C1H4)	Proteintech	CAT#60293-1-Ig; RRID:AB_2881408
Rabbit recombinant monoclonal anti-SIGMAR1 (Clone D4J2E)	Cell Signaling Technology	CAT#61994; RRID:AB_2799617
Rabbit recombinant monoclonal anti-SOD1 (Clone EP1727Y) (Fluorescent Wb)	Abcam	CAT#ab51254; RRID:AB_882757
Rabbit polyclonal anti-SOD1 (Chemiluminescent Wb)	GeneTex	CAT#GTX100554; RRID:AB_10618670
Rabbit recombinant monoclonal anti-SQSTM1 (clone EPR4844) (Fluorescent Wb)	Abcam	CAT#ab109012; RRID: AB_2810880
Mouse monoclonal anti-SQSTM1 (clone 2C11) (Chemiluminescent Wb)	Abcam	CAT#ab56416; RRID: AB_945626
Rabbit recombinant monoclonal anti-TAF15 (clone JE61-92)	Thermo Fisher Scientific	CAT#MA5-44822; RRID: AB_2931279
Rabbit recombinant monoclonal anti-TARDBP (clone 11N20)	Proteintech	CAT#80001-1-RR; RRID: AB_2882933
Rabbit recombinant monoclonal anti-TBK1 (Clone EP611Y) (Chemiluminescent Wb)	Abcam	CAT#ab40676; RRID: AB_776632
Rabbit recombinant monoclonal anti-TBK1 (clone E8I3G) ((Fluorescent Wb)	Cell Signaling Technology	CAT#38066; RRID: AB_2827657
Rabbit recombinant monoclonal anti-TIA1 (Clone D1Q3K)	Cell Signaling Technology	CAT#86050; RRID: AB_2800070
Mouse monoclonal anti-UBQLN2 (clone 6H9) (Figure 4)	Abcam	CAT#ab190283; RRID: AB_2747782
Rabbit recombinant monoclonal anti-VCP (Clone 7F3) (Chemiluminescent Wb)	Cell Signaling Technology	CAT#2649; RRID:AB_2214629
Rabbit recombinant monoclonal anti-VCP (clone EPR3307(2)) (Fluorescent Wb)	Abcam	CAT#ab109240; RRID:AB_10862588
Rabbit polyclonal anti-ANXA11	Aviva Systems Biology	CAT#ARP87950_P050; RRID:AB_2894925
Mouse monoclonal anti-C9orf72 (clone GT1553)	GeneTex	CAT#GTX634482; RRID:AB_2784545
Rabbit polyclonal anti-CHCHD10 (Chemiluminescent Wb)	Proteintech	CAT#25671-1-AP; RRID:AB_2880187
Mouse monoclonal anti-CHCHD10 (clone OTI3B8) (Fluorescent Wb)	Thermo Fisher Scientific	CAT#MA5-27535; RRID:AB_2724132
Rabbit recombinant monoclonal anti-LGALS1 (clone EPR3206(2))	Abcam	CAT#ab138513; RRID:AB_2894851
Rabbit recombinant monoclonal anti-PFN1 (clone ARC1469)	ABclonal	CAT#A9188; RRID:AB_2863682
Rabbit recombinant monoclonal anti-SPG11 (clone 2H25L11)	Thermo Fisher Scientific	CAT#702776; RRID:AB_2725406
Mouse monoclonal anti-ACSL5 (Clone 5H8)	Abnova	CAT#H00051703-M01; RRID:AB_509241
Rabbit recombinant monoclonal anti-CAV1 (clone SZ02-01) (Chemiluminescent Wb)	Thermo Fisher Scientific	CAT#MA5-32020; RRID:AB_2809314
Rabbit recombinant monoclonal anti-CAV1 (Clone ARC50848) (Fluorescent Wb)	ABclonal	CAT#A19006; RRID:AB_2862498

Rabbit recombinant monoclonal anti-ATXN2 (clone EPR23630-49)	Abcam	CAT#ab254362; RRID:AB_2885130
Rabbit recombinant monoclonal anti-TUBA4A (Clone EPR13478(B)) (Chemiluminescent Wb)	Abcam	CAT#ab176560; RRID: AB_2860019
Rabbit recombinant monoclonal anti-TUBA4A (Clone JM73-24) (Fluorescent Wb)	Thermo Fisher Scientific	CAT#MA5-32738; RRID: AB_2810015
Rabbit recombinant monoclonal anti-VAPB (clone EPR27026-50) (Chemiluminescent Wb)	Abcam	CAT#ab315013; RRID:AB_3086770
Rabbit polyclonal anti-VAPB (Fluorescent Wb)	Thermo Fisher Scientific	CAT#PA5-53023; RRID:AB_2649391
Rabbit recombinant monoclonal anti-ALS2 (clone EPR11185)	Abcam	CAT#ab170896; RRID:AB_2885099
Mouse monoclonal anti-HNRNPA2B1 (clone DP3B3)	Bio-Techne (Novus Biologicals)	CAT#NB120-6102; RRID:AB_790226
Rabbit recombinant monoclonal anti-KIF5A (clone 241124H1)	Proteintech	CAT# 84013-4-RR; RRID: AB_3671581
Rabbit recombinant monoclonal anti-Synaptotagmin 1 (clone HL1626)	GeneTex	CAT# GTX637119; RRID: AB_3068350
Rabbit recombinant monoclonal anti-CD44 (clone EPR18668)	Abcam	CAT# ab189524; RRID: AB_2885107
Rabbit recombinant monoclonal anti-Islet 1 (Clone EPR10362)	Abcam	CAT# ab178400; RRID:AB_2927537
Rat recombinant monoclonal anti-Myelin Basic Protein antibody (clone 12)	Abcam	CAT#ab7349; RRID: AB_305869
Rabbit polyclonal anti-Tyrosine Hydroxylase	Pel-Freeze	CAT# P40101-150: RRID: AB_2617184
Rabbit recombinant monoclonal anti-CD11b (clone EPR1344)	Abcam	CAT#ab133357; RRID: AB_2650514
Rabbit recombinant monoclonal anti- Iba1 (clone E4O4W)	Cell Signaling Technology	CAT#17198; RRID: AB_2820254
Other reagents		
Astrocyte Growth Supplements (AGS)	ScienCell Research Laboratories	CAT#1852
Astrocyte Medium (AM)	ScienCell Research Laboratories	CAT#1801-b
BLUelf Prestained Protein Ladder	FroggaBio	CAT#PM008
CellTracker deep red dye	Thermo Fisher Scientific	CAT#C34565
CellTracker green chloromethyl derivative of fluorescein diacetate (CMFDA) dye	Thermo Fisher Scientific	CAT#C2925
Centrifugal filter unit, Amicon Ultra-15	MilliporeSigma	CAT#UFC901096
Interferon γ (IFNγ)	Peprotech	CAT#300-02
Interleukin 4 (IL-4)	Peprotech	CAT#200-04
Lipopolysaccharide (LPS)	Thermo Fisher	CAT#00-4976-93
mTeSR1	STEMCELL Technologies	CAT#85850
NuPAGE™ Bis-Tris Midi Protein Gels, 10%, 1.0 mm	Thermo Fisher Scientific	CAT#WG1201BOX
NuPAGE™ MES SDS Running Buffer (20X)	Thermo Fisher Scientific	CAT#NP000202
NuPAGE™ MOPS SDS Running Buffer (20X)	Thermo Fisher Scientific	CAT#NP000102
PhenoPlate, 96-well, optically clear flat bottom	Perkin Elmer	CAT#6055300
Pierce™ IP Lysis Buffer	Thermo Fisher Scientific	CAT#87788
RIPA Lysis and Extraction Buffer	Thermo Fisher Scientific	CAT#89901
STEMdiff™ Forebrain Neuron Differentiation Kit	STEMCELL Technologies	CAT#08600
STEMdiff™ Forebrain Neuron Maturation Kit	STEMCELL Technologies	CAT#08605
STEMdiff™ Hematopoietic Kit	STEMCELL Technologies	CAT#05310
STEMdiff™ Hematopoietic Kit	STEMCELL Technologies	CAT#05310
STEMdiff™ Hematopoietic Kit	STEMCELL Technologies	CAT#05310
Experimental models: Cell lines		

Healthy control iPSCs from the AIW002-02 background	EDDU, McGill University	NA
Healthy control iPSCs from the QPN929 background	EDDU, McGill University	NA
Software and algorithms		
LI-COR Image Studio Lite	licorbio.com/image-studio	NA
FIJI Software	fiji.sc/	RRID:SCR_002285
MetaXpress High-Content Screening Software version 6.7.1.157	moleculardevices.com/products/cellular-imaging-systems/high-content-analysis/metaxpress - overview	RRID:SCR_016654
PyCharm 2023.3.4	jetbrains.com/pycharm/	RRID:SCR_018221
RStudio 2023.09.1	cran.rstudio.com/	RRID:SCR_000432
Other		
Antibody Registry	antibodyregistry.org	RRID:SCR_006397
Cellosaurus - a knowledge resource on cell lines	cellosaurus.org	RRID:SCR_013869
CiteAb - Reagent Search & Life Science Data	citeab.com	RRID:SCR_009653
ClinGen	https://clinicalgenome.org/	RRID:SCR_014968
DepMap: The Cancer Dependency Map Project at Broad Institute	depmap.org/portal	RRID:SCR_017655
PubMed	pubmed.ncbi.nlm.nih.gov	RRID:SCR_004846
Structural Genomics Consortium	https://www.thesgc.org/	RRID:SCR_003890
The Human Protein Atlas	proteinatlas.org	RRID:SCR_006710
Zenodo	https://zenodo.org/	RRID:SCR_004129

References

1. Leonard HL, Global Parkinson's Genetics P. Novel Parkinson's Disease Genetic Risk Factors Within and Across European Populations. *medRxiv*. Mar 17 2025;doi:10.1101/2025.03.14.24319455

2. Kim JJ, Vitale D, Otani DV, et al. Multi-ancestry genome-wide association meta-analysis of Parkinson's disease. *Nat Genet*. Jan 2024;56(1):27-36. doi:10.1038/s41588-023-01584-8

3. Bellenguez C, Kucukali F, Jansen IE, et al. New insights into the genetic etiology of Alzheimer's disease and related dementias. *Nat Genet*. Apr 2022;54(4):412-436. doi:10.1038/s41588-022-01024-z

4. Zhang J, Wang Y, Zhang Y, Yao J. Genome-wide association study in Alzheimer's disease: a bibliometric and visualization analysis. *Front Aging Neurosci*. 2023;15:1290657. doi:10.3389/fnagi.2023.1290657

5. van Rheenen W, van der Spek RAA, Bakker MK, et al. Common and rare variant association analyses in amyotrophic lateral sclerosis identify 15 risk loci with distinct genetic architectures and neuron-specific biology. *Nat Genet*. Dec 2021;53(12):1636-1648. doi:10.1038/s41588-021-00973-1

6. Nijs M, Van Damme P. The genetics of amyotrophic lateral sclerosis. *Curr Opin Neurol*. Oct 1 2024;37(5):560-569. doi:10.1097/WCO.0000000000001294

7. Go CD, Knight JDR, Rajasekharan A, et al. A proximity-dependent biotinylation map of a human cell. *Nature*. Jul 2021;595(7865):120-124. doi:10.1038/s41586-021-03592-2

8. Bajc Cesnik A, Motaln H, Rogelj B. The Impact of ALS-Associated Genes hnRNPA1, MATR3, VCP and UBQLN2 on the Severity of TDP-43 Aggregation. *Cells*. Jul 28 2020;9(8)doi:10.3390/cells9081791

9. Johnson JO, Pioro EP, Boehringer A, et al. Mutations in the Matrin 3 gene cause familial amyotrophic lateral sclerosis. *Nat Neurosci*. May 2014;17(5):664-666. doi:10.1038/nn.3688

10. Monteiro FL, Voskuil JLA, Williams C. YCharOS protocol for antibody validation. *Nat Protoc*. Jun 2025;20(6):1389-1390. doi:10.1038/s41596-024-01108-6

11. Ayoubi R, Ryan J, Gonzalez Bolivar S, et al. A consensus platform for antibody characterization. *Nat Protoc*. Dec 17 2024;doi:10.1038/s41596-024-01095-8

12. Ayoubi R, Ryan J, Biddle MS, et al. Scaling of an antibody validation procedure enables quantification of antibody performance in major research applications. *Elife*. Nov 23 2023;12doi:10.7554/eLife.91645

13. Hornsby M, Paduch M, Miersch S, et al. A High Through-put Platform for Recombinant Antibodies to Folded Proteins. *Mol Cell Proteomics*. Oct 2015;14(10):2833-47. doi:10.1074/mcp.O115.052209

14. Biddle M, Stylianou P, Rekas M, et al. Improving the integrity and reproducibility of research that uses antibodies: a technical, data sharing, behavioral and policy challenge. *MAbs*. Jan-Dec 2024;16(1):2323706. doi:10.1080/19420862.2024.2323706

15. Rehm HL, Berg JS, Brooks LD, et al. ClinGen--the Clinical Genome Resource. *N Engl J Med*. Jun 4 2015;372(23):2235-42. doi:10.1056/NEJMsr1406261

16. Marx V. Change-makers bring on recombinant antibodies. *Nat Methods*. Aug 2020;17(8):763-766. doi:10.1038/s41592-020-0915-8

17. Marcon E, Jain H, Bhattacharya A, et al. Assessment of a method to characterize antibody selectivity and specificity for use in immunoprecipitation. *Nat Methods*. Aug 2015;12(8):725-31. doi:10.1038/nmeth.3472

18. Bandrowski A, Pairish M, Eckmann P, Grethe J, Martone ME. The Antibody Registry: ten years of registering antibodies. *Nucleic Acids Res*. Jan 6 2023;51(D1):D358-D367. doi:10.1093/nar/gkac927

19. Bairoch A. The Cellosaurus, a Cell-Line Knowledge Resource. *J Biomol Tech*. Jul 2018;29(2):25-38. doi:10.7171/jbt.18-2902-002

20. Ayoubi R, McDowell I, Fotouhi M, et al. The identification of high-performing antibodies for Profilin-1 for use in Western blot, immunoprecipitation and immunofluorescence. *F1000Res*. 2023;12:348. doi:10.12688/f1000research.132249.1

21. Cai Z, Yin K, Liu Q, Liu M, Yang X, Cui L. Association between abnormal expression and methylation of LGALS1 in amyotrophic lateral sclerosis. *Brain Res*. Oct 1 2022;1792:148022. doi:10.1016/j.brainres.2022.148022

22. Kato T, Kurita K, Seino T, et al. Galectin-1 is a component of neurofilamentous lesions in sporadic and familial amyotrophic lateral sclerosis. *Biochem Biophys Res Commun*. Mar 23 2001;282(1):166-72. doi:10.1006/bbrc.2001.4556

23. Karlsson M, Zhang C, Mear L, et al. A single-cell type transcriptomics map of human tissues. *Sci Adv*. Jul 2021;7(31)doi:10.1126/sciadv.abh2169

24. McKeever PM, Sababi AM, Sharma R, et al. Single-nucleus transcriptome atlas of orbitofrontal cortex in ALS with a deep learning-based decoding of alternative polyadenylation mechanisms. *Cell Genom*. Sep 17 2025:101007. doi:10.1016/j.xgen.2025.101007

25. Gygi SP, Rochon Y, Franza BR, Aebersold R. Correlation between protein and mRNA abundance in yeast. *Mol Cell Biol*. Mar 1999;19(3):1720-30. doi:10.1128/MCB.19.3.1720

26. Vogel C, Marcotte EM. Insights into the regulation of protein abundance from proteomic and transcriptomic analyses. *Nat Rev Genet*. Mar 13 2012;13(4):227-32. doi:10.1038/nrg3185

27. Michaelis T, Lindestam Arlehamn CS, Johansson E, et al. Autoimmune response to C9orf72 protein in amyotrophic lateral sclerosis. *Nature*. Oct 1 2025;doi:10.1038/s41586-025-09588-6

28. Siletti K, Hodge R, Mossi Albiach A, et al. Transcriptomic diversity of cell types across the adult human brain. *Science*. Oct 13 2023;382(6667):eadd7046. doi:10.1126/science.add7046

29. Deneault E, Chaineau M, Nicouleau M, et al. A streamlined CRISPR workflow to introduce mutations and generate isogenic iPSCs for modeling amyotrophic lateral sclerosis. *Methods*. Jul 2022;203:297-310. doi:10.1016/j.ymeth.2021.09.002

30. Lepine S, Nauleau-Javaudin A, Deneault E, et al. Homozygous ALS-linked mutations in TARDBP/TDP-43 lead to hypoactivity and synaptic abnormalities in human iPSC-derived motor neurons. *iScience*. Mar 15 2024;27(3):109166. doi:10.1016/j.isci.2024.109166

31. Kriks S, Shim JW, Piao J, et al. Dopamine neurons derived from human ES cells efficiently engraft in animal models of Parkinson's disease. *Nature*. Nov 6 2011;480(7378):547-51. doi:10.1038/nature10648

32. C XQC, Deneault E, Abdian N, et al. Generation of patient-derived pluripotent stem cell-lines and CRISPR modified isogenic controls with mutations in the Parkinson's associated GBA gene. *Stem Cell Res*. Oct 2022;64:102919. doi:10.1016/j.scr.2022.102919

33. Piscopo VEC, Chapleau A, Blaszczyk GJ, et al. The use of a SOX10 reporter toward ameliorating oligodendrocyte lineage differentiation from human induced pluripotent stem cells. *Glia*. Jun 2024;72(6):1165-1182. doi:10.1002/glia.24524

34. Soubannier V, Chaineau M, Gursu L, et al. Rapid Generation of Ventral Spinal Cord-like Astrocytes from Human iPSCs for Modeling Non-Cell Autonomous Mechanisms of Lower Motor Neuron Disease. *Cells*. Jan 24 2022;11(3)doi:10.3390/cells11030399

35. McQuade A, Coburn M, Tu CH, Hasselmann J, Davtyan H, Blurton-Jones M. Development and validation of a simplified method to generate human microglia from pluripotent stem cells. *Mol Neurodegener*. Dec 22 2018;13(1):67. doi:10.1186/s13024-018-0297-x

A

gene name	number of antibodies tested	cell line background(s)	WB	IP	IF
ACSL5	8	HCT116	●	●	□
ALS2	3	HAP1	●	●	—
ANG	3	HAP1	□	—	—
ANXA11	15	HeLa	●	●	⬡
ATXN2	5	HAP1	●	●	□
C9orf72	16	U2OS	●	●	●
CAV1	17	U87mg	●	—	—
CCNF	3	U2OS	●	—	—
CHCHD10	4	HAP1	●	●	●
CHMP2B	8	U2OS	●	●	●
FIG4	5	HAP1	●	□	—
FUS	10	HeLa	●	●	●
HNRNPA1	6	HEK293T	●	⬡	●
HNRNPA2B1	8	HAP1	●	●	●
KIF5A	4	U2OS	●	—	—
LGALS1	11	HAP1	●	●	●
MATR3	4	HAP1	●	●	●
NEK1	9	HeLa	●	—	—
OPTN	8	U2OS	●	●	●
PFN1	16	HAP1	●	●	●
SETX	11	RKO	●	—	—
SIGMAR1	5	HeLa, HEK293T	●	—	—
SOD1	11	HeLa	●	●	●
SPG11	3	HAP1	●	—	—
SQSTM1	17	U2OS	●	●	●
TAF15	5	HAP1	●	●	●
TARDBP	18	HAP1	●	●	●
TBK1	11	U2OS	●	●	●
TIA1	12	HAP1	●	●	●
TUBA4A	6	HeLa, HAP1	●	●	●
UBQLN2	10	HAP1	●	●	●
VAPB	6	HeLa	●	●	●
VCP	16	U2OS	●	●	●

● Specific, renewable antibody identified
□ Specific, polyclonal antibody identified
⬡ No specific antibodies identified
— Application not tested or inconclusive

B

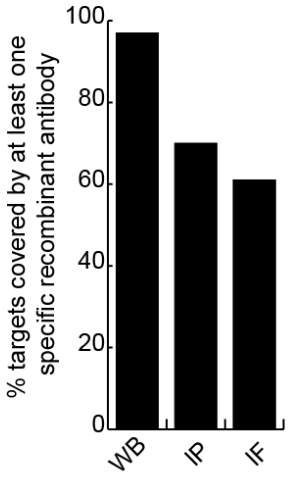

C

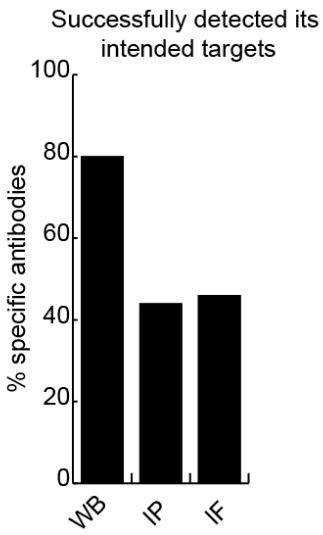

Ayoubi et al., Figure 1

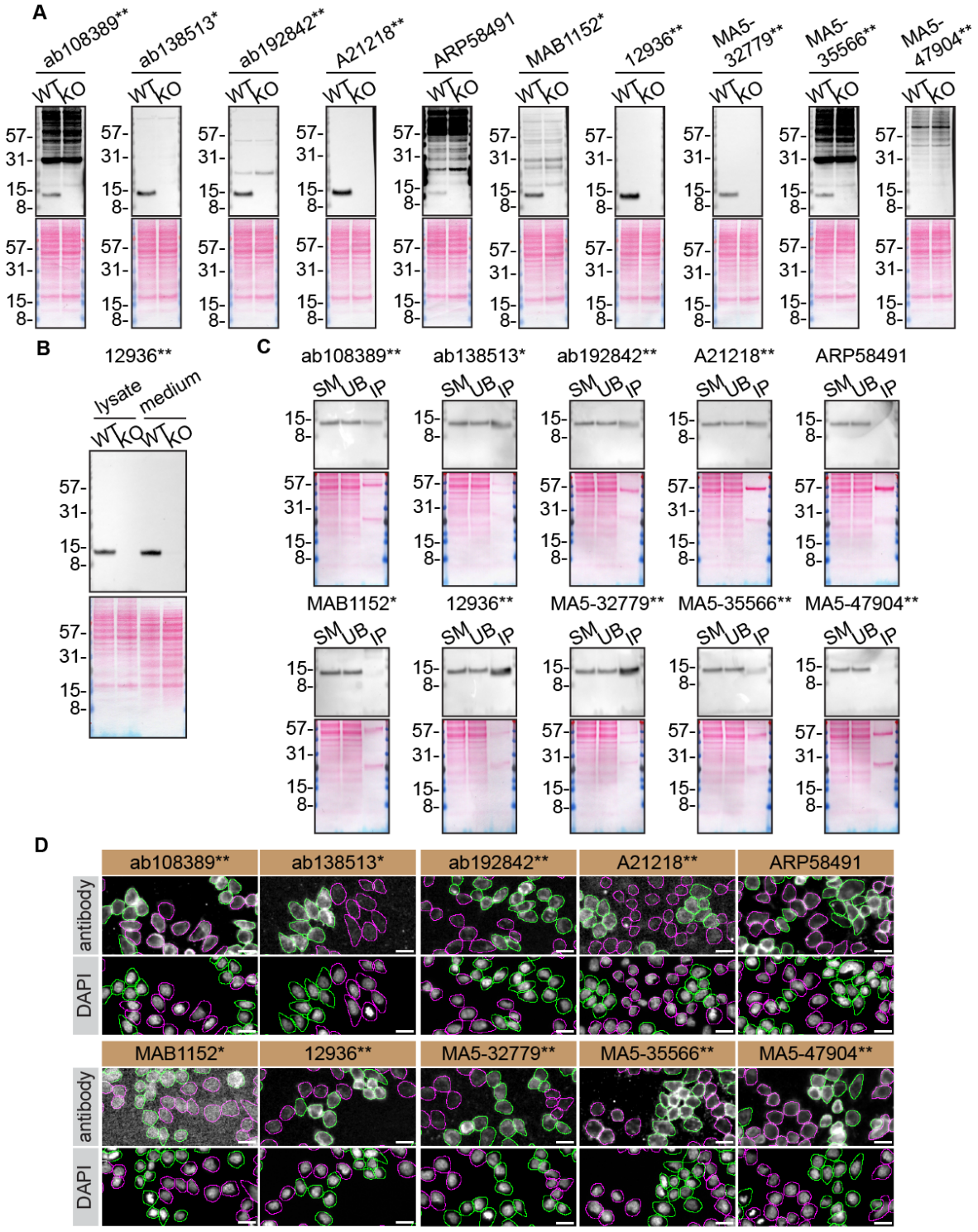

Ayoubi et al., Figure 2

A

B

	number of tested antibodies
no applied filter	10

	application	number of recommended antibodies
applied filter	WB	5
	IP	5
	IF	4

Ayoubi et al., Figure 3

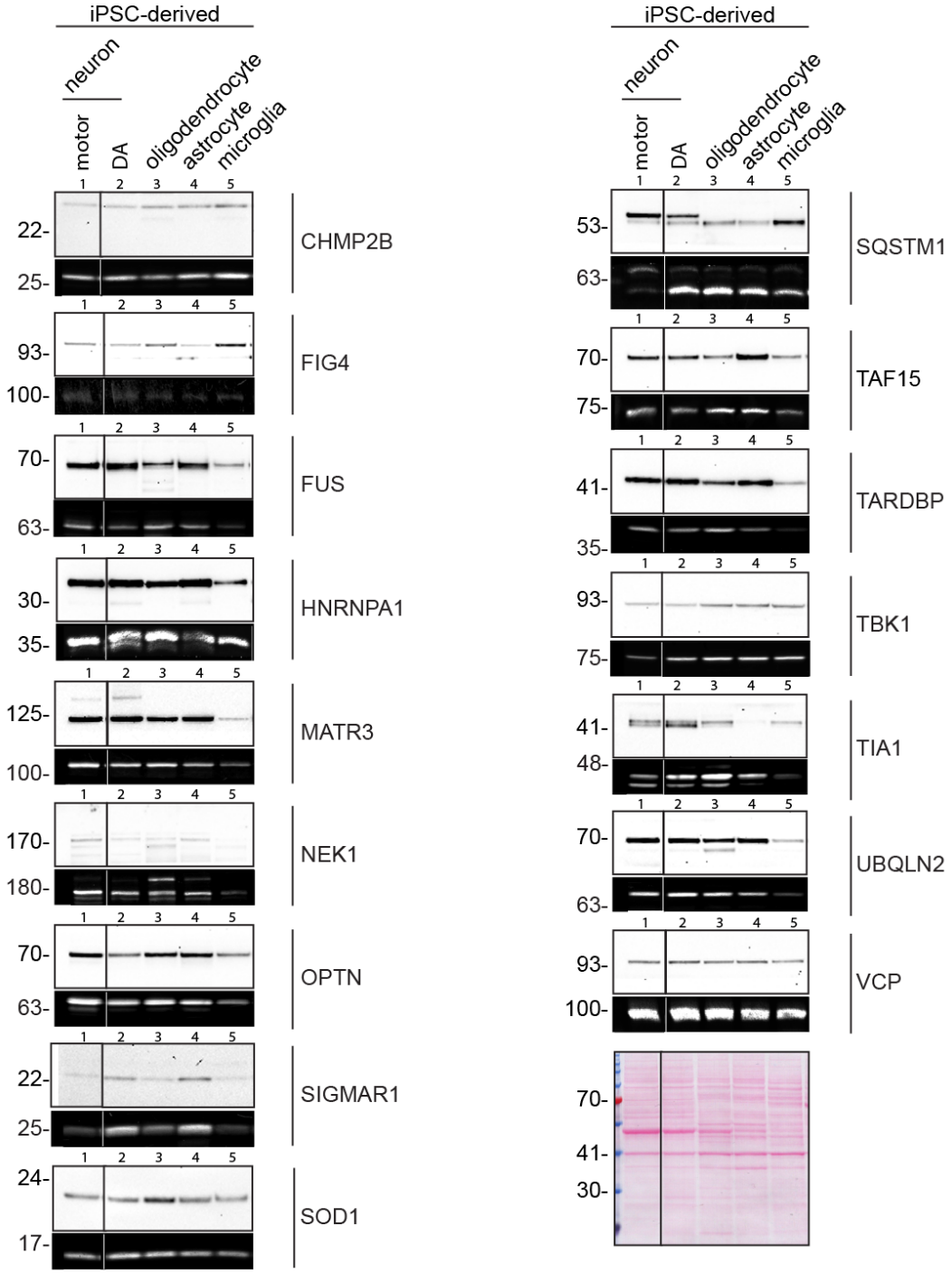

Ayoubi et al., Figure 4

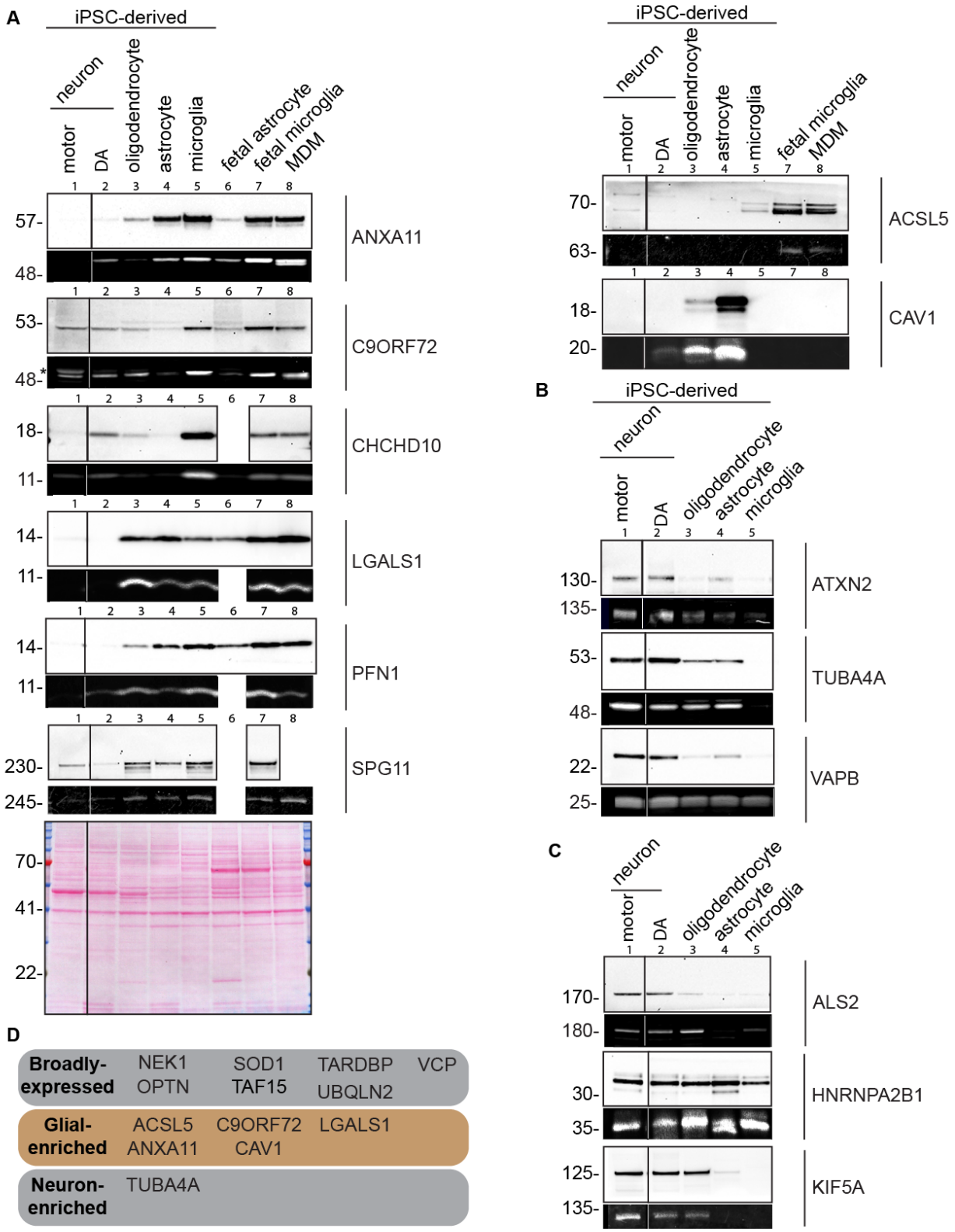

Ayoubi et al., Figure 5

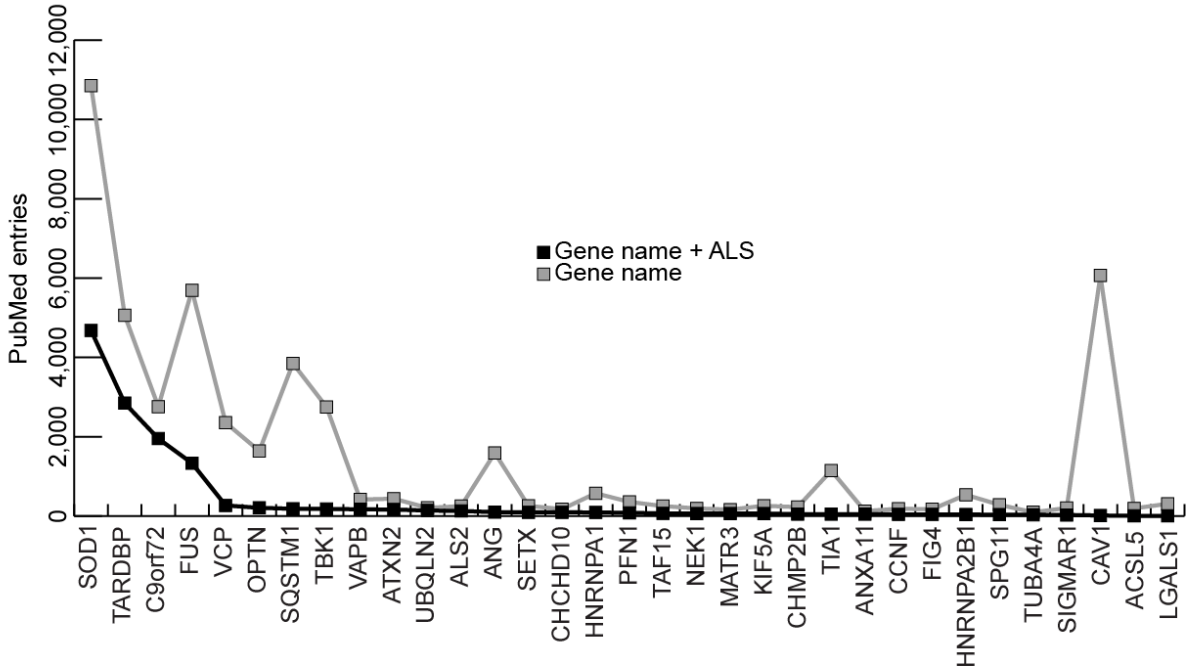

Ayoubi et al., Figure S1

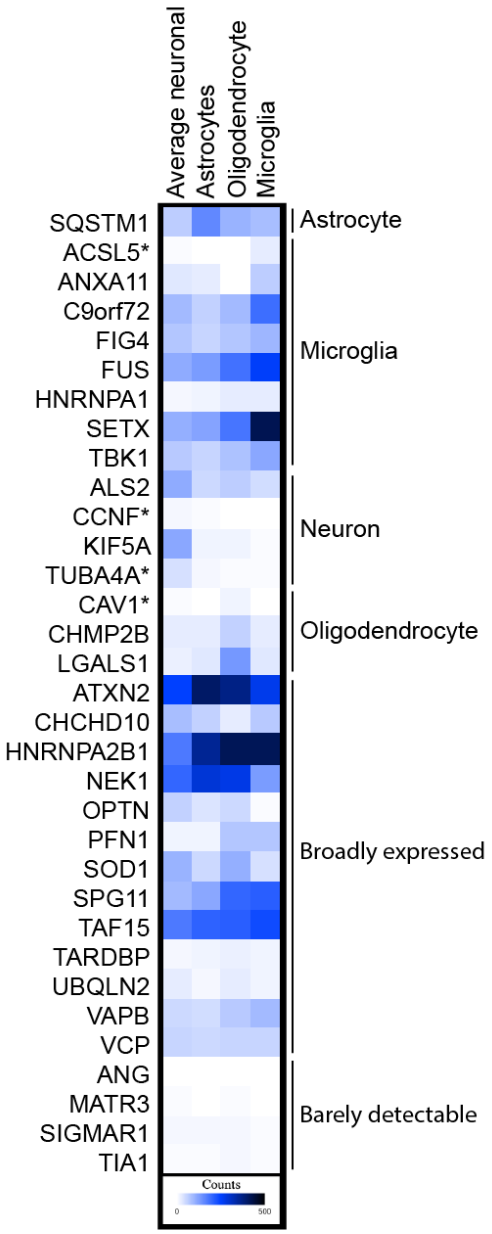

Ayoubi et al., Figure S2

A

neuronal	SYT1
glial	CD44
motor neuron	ISL1
dopaminergic neuron	TH
oligodendrocyte	MBP
astrocyte	GFAP
microglia	CD11b IBA1

B

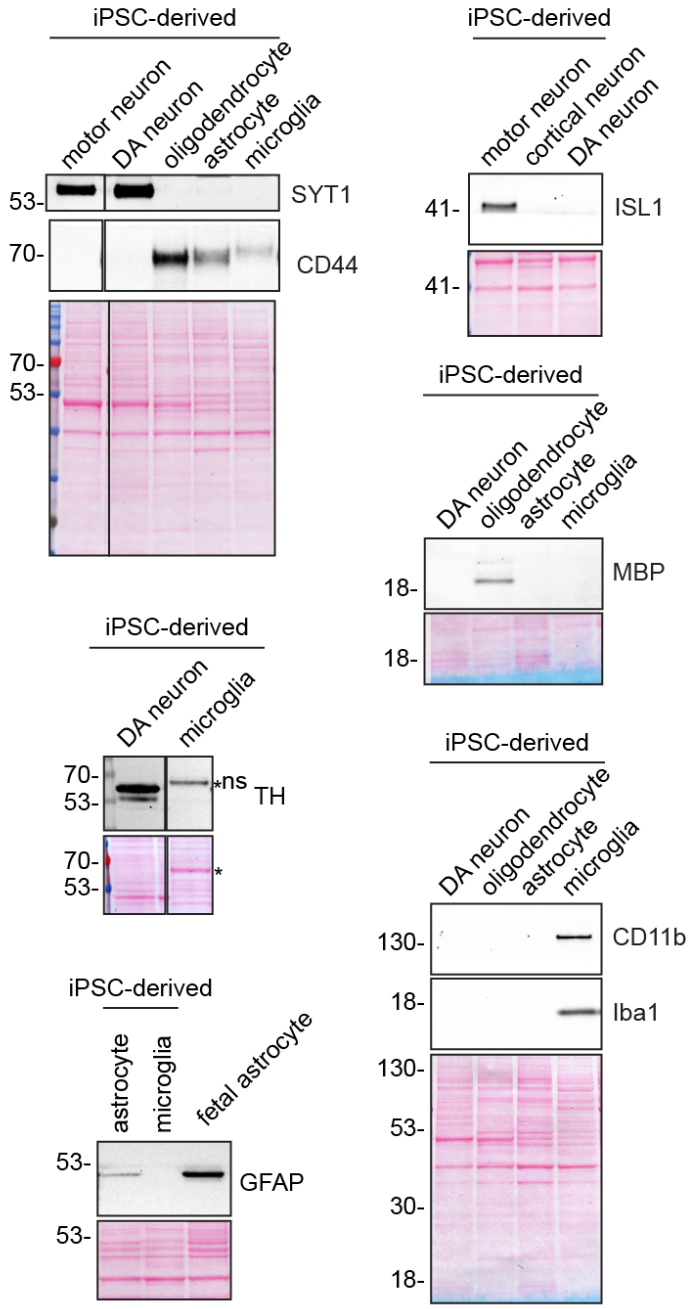

Ayoubi et al., Figure S3

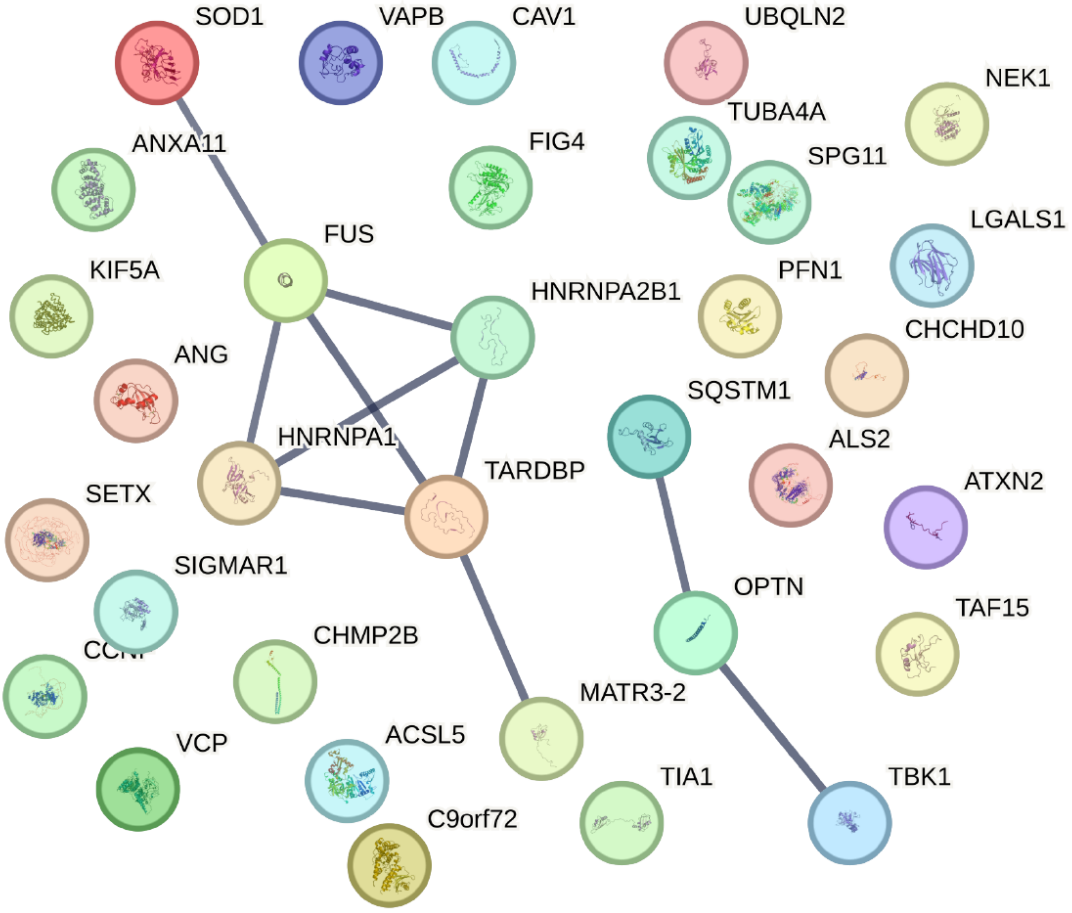

Ayoubi et al., Figure S4